Investigations of a Binary Asteroid Dynamical Model

Nicholas J. Freeman

A senior thesis submitted to the faculty of
Brigham Young University
in partial fulfillment of the requirements for the degree of

Bachelor of Science

Lennard Bakker and Darin Ragozzine, Advisor

Department of Physics and Astronomy

Brigham Young University

April 2023

ABSTRACT

Investigations of a Binary Asteroid Dynamical Model

Nicholas J. Freeman
Department of Physics and Astronomy, BYU
Bachelor of Science

Asteroids and other small objects throughout the Solar System are known to exhibit many of the oddities of classical Newtonian gravitation, and these oddities vastly increase the difficulty of analysis in N-body modeling and simulation. Recently, there has been developments in the study of binary asteroids which orbit each other simultaneously in the broader Sun-Planet field. We use a modified four-body model to analyze the evolution of two asteroids in a broader field of two primaries of arbitrary mass. We show the existence of relative equilibria and periodic orbits of Hill, Comet, Lyapunov, and Binary type in our model. We also present the spectra of the reported equilibria.

Keywords: 4-body problem, binary asteroids, relative equilibria, periodic orbits, Hamiltonian dynamical systems

ACKNOWLEDGMENTS

I would like to thank Dr. Lennard Bakker for his constant help in my learning the requisite theory and proof techniques needed for this work, as well as his elaboration on the details of the relative equilibria results. I am also especially grateful for the funding I received for my research through the College of Physical and Mathematical Sciences and Mathematics department of Brigham Young University, and by extension the donors who enable paid research.

Contents

List of Figures

Chapter 1

Introduction

Since its inception, Newtonian gravitation has challenged physicists and mathematicians alike in understanding the motion of the heavens. The simplicity of the $1/r^2$ force law means that the differential equations underlying Newtonian gravity are relatively easy to write down and understand. These equations define the N-body problem, the model for the motion of N masses undergoing mutual gravitational attraction. However, finding the solutions of the N-body problem has proven to be a very difficult task. Very few particular "closed-form" solutions are known except in the $N = 2$ case (cf. Meyer & Offin Chapter 3 [1] or Taylor Chapter 8 [2]), and no general framework exists for any larger N.

1.1 The N-Body Problem

The inability to solve the differential equations underlying the N-body problem generally has not stopped the broader community from obtaining new information about the stability/instability of certain dynamics. For example, the well-studied “circular restricted 3-body problem" (CR3BP, cf. Meyer & Offin Chapter 4 [1]) predicts the existence of five Lagrange points (see Figure 1.1) where small masses like asteroids and satellites can sit unperturbed. These predictions have led to

the discovery of the Jupiter Trojan asteroids as well as the placement of the James Webb Space Telescope and of ESA's Gaia probe.

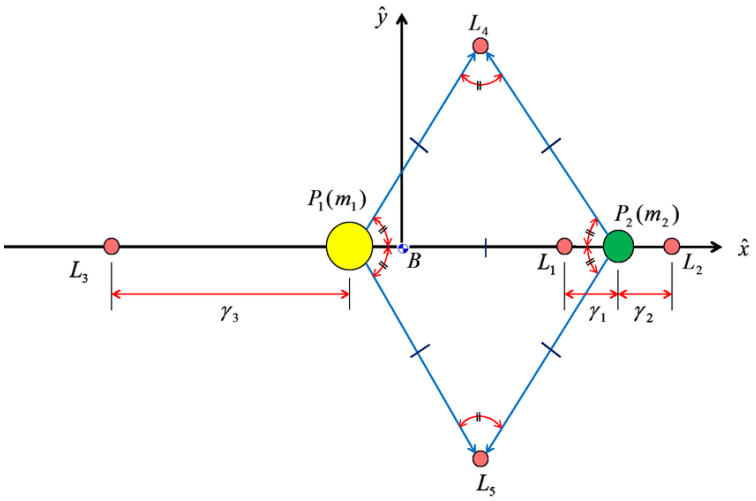

Figure 1.1 Depiction of the five Lagrange points (labeled $L_1, \cdots, L_5$) defined by two masses (yellow and green) orbiting each other in circular trajectories. The coordinate frame turns with the masses to match their rotation, so that any small particle placed with sufficient momentum at any L_i will remain there.

Other dynamical oddities of the N-body problem present themselves under specific mass, position, and momentum configurations. Such configurations typically admit exploitable symmetries which allow for more careful analysis of the geometry of solutions. Indeed, in this thesis we shall consider an intuitive reduction of the full 4-body problem pertaining to the dynamics of small "binary asteroids" in the gravity of the Sun and a planet. Our model will introduce some configuration symmetries necessary for useful analysis.

1.2 Hamiltonian Dynamical Systems

The language of the theory behind N-body problem analysis is that of Hamiltonian dynamical systems. Pioneered by Sir William Rowan Hamilton [3], Hamiltonian dynamics originally served to reformulate Newton's mechanics in such a way to simply record and solve equations of motion

using the "total energy" of the system. Due to this simplicity, the theory has since evolved to cover any and all systems of differential equations whose structure is derived from a "Hamiltonian function" (the abstraction of the total energy to non-physical systems).

The core mathematics behind a Hamiltonian dynamical system is thus: suppose we have a generalized position coordinate $q(t)$ for a particle and a corresponding generalized momentum coordinate $p(t)$. Suppose the total energy (i.e., kinetic plus potential) of the particle is expressible as a function $H(q,p,t)$ of q, p, and time t. Then the equations of motion for this particle are

$$\frac{dq}{dt} = \frac{\partial H}{\partial p}, \ \frac{dp}{dt} = -\frac{\partial H}{\partial q}. \tag{1.1}$$

More generally, given an evolving system of particles with complete generalized coordinates $q_i(t)$ and $p_i(t)$, the form of Eqn. (1.1) is repeated for each coordinate, and the Hamiltonian H becomes a function of every single coordinate. For example in our case, the masses in the N-body problem each have six generalized coordinates in 3-D: three position and three momentum. This makes $6N$ copies of Eqn. (1.1), which means the full 4-body problem alone has 24 equations.

To illustrate a basic system, the equation of motion for a simple harmonic oscillator in one dimension (cf. Taylor Chapter 5 [2]), $m\ddot{q} = -kq$, is expressible in the Hamiltonian language using the momentum coordinate $p = m\dot{q}$ and Hamiltonian

$$H_{SHO}(q,p) = \frac{1}{2}\left(\frac{p^2}{m} + kq^2\right),$$

which yields $\dot{q} = p/m$ and $\dot{p} = -kq$ according to Eqn. (1.1). The harmonic oscillator displays a commonality found in many physical Hamiltonian systems: the kinetic energy is represented just by the momentum (the $p^2/2m$ term) while the potential energy is represented by the position (the kq^2 term).

This commonality persists in the Hamiltonian for the full N-body problem. Given masses $m_1, \cdots, m_N > 0$ at positions $q_i = (q_{x_i}, q_{y_i}, q_{z_i})$ with momenta $p_i = (p_{x_i}, p_{y_i}, p_{z_i})$, the Hamiltonian is

the total energy

$$H_N(q,p) = \sum_{i=1}^{N} \frac{\|p_i\|^2}{2m_i} - \sum_{1\le i<j\le N} \frac{m_i m_j}{\|q_i - q_j\|}. \tag{1.2}$$

Here we have chosen the time units so that the universal gravitation constant G is one, for simplicity. Throughout this thesis, we will refer to Eqn. (1.2) in the case $N = 4$, modifying it to suit our needs.

1.3 Binary Asteroids in the Solar System

This thesis is concerned with the evolution of "binary asteroids," which in our model are two small but positive mass particles moving in the broader gravitational field of one or more large particles. In particular, we investigate the motion of binary asteroids in a field of two "primaries" of larger mass and known trajectory. Such could be represented by the Sun and a planet like Earth or Jupiter.

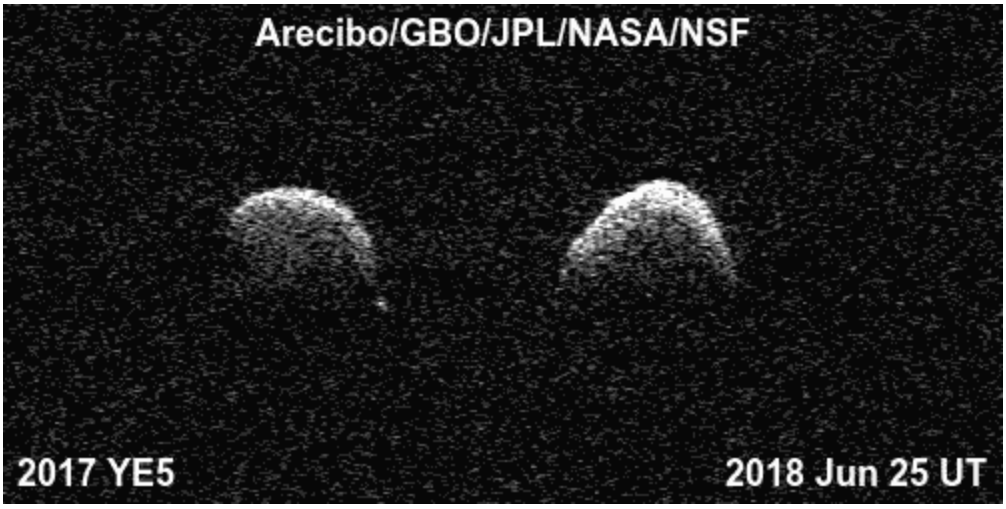

Figure 1.2 Radio image of the binary asteroid 2017 YE5 from Arecibo Observatory and the Green Bank Observatory. The two asteroids have similar shape and orbit each other. Image courtesy of Arecibo/GBO/NSF/NASA/JPL-Caltech.

The main Hamiltonian we will use throughout this work was developed by Lennard Bakker in response to the discovery of the real binary asteroid 2017 YE5 by Claudine Rinner in December 2017 (reported in [4]). This binary came close enough to Earth in June 2018 that ground-based

radio imaging revealed it was indeed a pair of asteroids (see Figure 1.2). The most remarkable property of 2017 YE5 is that the two asteroids have nearly equal mass. Only three other binary asteroids are known to have this property: 90 Antiope, 2006 VW 139, and 69230 Hermes [5].

Most other known binaries have a larger central mass, with a smaller companion. This is illustrated, for example, by the near-Earth binary Didymos and Dimorphos, which was the target of the NASA Double Asteroid Redirection Test (DART) mission in 2021. The objective of the DART mission was to experimentally determine how much the binary dynamics would be altered by a collision with the mission spacecraft. Once the craft arrived to the binary in September 2022, the planned collision managed to change the orbital period by 33 minutes [6]. For comparison, the "mission success" threshold was 73 seconds [7].

The disparity between the DART success threshold and the actual orbital perturbation illustrates part of the difficulty in predicting binary dynamics: they are sensitive to small changes in the orbital conditions. While this may be comforting to scientists who seek to divert the trajectories of possibly dangerous large asteroids away from Earth, it means that modeling requires great precision in its treatment of various effects. Nevertheless, some qualitative (and quantitative) behavior can be determined, and this is the challenge of theorists.

1.4 Outline of Thesis

The objective of this thesis is to present a planar (i.e., 2-D) 4-body problem for the motion of binary asteroids in the field of two large primaries. We report findings of dynamical similarities between our model and other existing adaptations of the N-body problem, including the aforementioned CR3BP (as presented in Meyer & Offin [1]), as well as other "restricted" 4-body problems such as the equal primary, collinear central configuration model in Llibre et al. [8], and the equilateral model in Alvarez-Ramírez et al. [9].

In Chapter 2, we lay some necessary background behind Hamiltonian dynamical systems theory. This includes the technique of implementing "symplectic coordinate changes" to simplify the equations of motion (1.1), as well as the statements of major dynamical "continuation" theorems. These theorems pertain to the existence and spectral stability of relative equilibrium configurations and periodic orbits. We will also present the relevant Hamiltonians used in our analyses.

Chapter 3 contains graphs of several different orbits obtained using Runge-Kutta solvers in MATLAB. These orbits motivate and illustrate the general analytical results discussed in Chapters 4 and 5.

Chapter 4 presents the first analytical results. This chapter pertains to the determination of equilibrium configurations when the two members of the two pairs of bodies have equal mass within the pair. We find that this restriction introduces a "center-of-mass" integral into the system, allowing us to reduce the degrees of freedom of the equations of motion (1.1). This thereby transforms the system into a Hamiltonian system reminiscent of Llibre, Paşca, and Valls' collinear circular restricted 4-body problem [8]. Therefore, we find six relative equilibria corresponding to their results and to the points in the CR3BP (see Figure 1.1; L_1 is represented twice). We report that the four configurations on the line of syzygy are unstable Lyapunov centers whereas the two off-axis configurations are hyperbolically unstable.

Chapter 5 is divided into two parts. The first part continues the equal-pair restriction from Chapter 4 in analyzing Hill-type periodic orbits, where the asteroids either orbit the primaries separately or they orbit each other at the system barycenter. The second part of this chapter removes the equal-pair restriction and examines comet-type periodic orbits, where both asteroids orbit far away from the primaries. The comet orbits persist for all physically reasonable choices of the four masses.

In, Chapter 6, we shall give some concluding remarks regarding the continuation of this research into several open problems. The two major points of consideration are adaptation into a full 3-D

Hamiltonian, and a "binary scaling" that forces the asteroids to move extremely closely together. In 3-D, we have some numerical evidence of periodic Hill orbits similar to those in Chapter 5, but there are issues with proving the corresponding theorems. For the binary scaling, we qualitatively present periodic orbits about each of the Lagrange points on the line of syzygy. While we have numerical evidence of similar quasi-periodic orbits about L_4 and L_5, this evidence is muddied by the possible presence of nearby full 4-body convex relative equilibria, like those presented in Corbera, Cors, & Roberts [10].

Chapter 2

Overview of Theory

The theory of Hamiltonian dynamics is rich in its own right, and we will only be able to present a very small amount relevant to this work. This chapter is divided into three parts, one for each major concept needed for the development of our results.

Section 2.1 begins with the most powerful technique of this thesis: developing symplectic coordinate changes within a Hamiltonian system. Such coordinate changes utilize the Chain Rule to edit the differential equations of motion into more favorable forms. However, to preserve the Hamiltonian character of the equations, we are constrained to the following trade-off: every edit to the position coordinates must be reflected by a similar edit to the momentum coordinates.

In this work, we make use of three main symplectic coordinate changes. First is a rotating reference frame which allows us to completely ignore the motion of the primaries mentioned in Section 1.3, thus reducing the number of equations to solve. Second is symplectic polar coordinates. These contain the well-known (r, θ) position coordinates as well as less-known momentum coordinates. Finally, we consider symplectic scalings. These allow us to "zoom in" or "out" to make specific gravitational forces more or less dominant. That way we can analyze the dynamics caused by one source at a time.

Section 2.2 presents the Hamiltonians and their associated equations of motion in the form of

Eqn. (1.1). First we shall revisit the 4-body problem (Eqn. (1.2) in the case $N = 4$) in the rotating reference frame of Section 2.1. The rotating coordinates introduce a nondissipative Coriolis effect into the total energy, which must be accounted for in the Hamiltonian. Next we derive the Binary Asteroid Hamiltonian developed by Lennard Bakker. Finally, we present the "center-of-mass" or COM reduction of the Binary Asteroid Hamiltonian. This final Hamiltonian restricts the masses of the system so to introduce a symmetry which cuts the number of equations to solve in half.

Section 2.3 gives the statements of "continuation" theorems as presented in Meyer & Offin [1]. These theorems essentially state the conditions when the dynamics of any system of differential equations persist under perturbation. These theorems couple with the symplectic scalings of Section 2.1 to give us our major results about relative equilibria and periodic orbits.

2.1 Symplectic Coordinates

Consider a system (physical or otherwise) characterized by n generalized position coordinates. If this system is Hamiltonian, then there are n more momentum coordinates, leading to n copies of Eqn. (1.1) (or $2n$ equations in all). In fact, that expression can be written more compactly using the $2n \times 2n$ matrix J_n given by

$$J_n = \begin{bmatrix} 0 & I_n \\ -I_n & 0 \end{bmatrix} \tag{2.1}$$

in block form, where I_n denotes the $n \times n$ identity matrix. One may check that $J_n^2 = I_{2n}$. This turns Eqn. (1.1) into

$$\dot{z} = J_n \nabla_z H(z,t) \tag{2.2}$$

where $z = (q_1, \cdots, q_n, p_1, \cdots, p_n)$, H is the Hamiltonian, and ∇_z denotes the gradient with respect to the coordinates of z only.

Coordinate changes (e.g., writing z in terms of a new variable $w = \Xi(z)$) in the system given by Eqn. (2.2) are called "symplectic" if the new equation of motion still has that form (albeit with a

new Hamiltonian H). Because the simplest form of coordinate change is a linear transformation, and differentiable functions can be locally approximated by their Jacobian matrix, we characterize general symplectic transformations in terms of matrices.

A $2n \times 2n$ matrix S is called symplectic if

$$SJ_nS^T = J_n.$$

Likewise, a diffeomorphism (invertible differentiable function whose inverse is also differentiable) $\Xi : \mathbb{R}^{2n} \to \mathbb{R}^{2n}$ is called symplectic if

$$[D\Xi(z)]J_n[D\Xi(z)]^T = J_n \tag{2.3}$$

for all $z \in \mathbb{R}^{2n}$. Here $D\Xi(z)$ is the Jacobian matrix

$$D\Xi(z) = \begin{bmatrix} \frac{\partial \Xi_1}{\partial z_1} & \cdots & \frac{\partial \Xi_1}{\partial z_{2n}} \\ \vdots & \ddots & \vdots \\ \frac{\partial \Xi_{2n}}{\partial z_1} & \cdots & \frac{\partial \Xi_{2n}}{\partial z_{2n}} \end{bmatrix}.$$

This applies to time-dependent transformations $\Xi(z,t)$ too–we simply add the stipulation that the condition Eqn. (2.3) holds for each fixed time t. In this case, if $w = \Xi(z,t)$ and we write the inverse as $z = Z(w,t)$, we can define a new Hamiltonian $\hat{H}(w,t) = H(Z(w,t),t)$. The Chain Rule applies to show that the new equations of motion are

$$\begin{aligned}
\dot{w} &= \frac{\partial \Xi}{\partial t}(z,t) + [D\Xi(z,t)]\dot{z} \\
&= \frac{\partial \Xi}{\partial t}(z,t) + [D\Xi(z,t)][J_n\nabla_z H(z,t)] \\
&= \frac{\partial \Xi}{\partial t}(z,t) + [D\Xi(z,t)]J_n[DH(z,t)]^T \\
&= \frac{\partial \Xi}{\partial t}(z,t) + [D\Xi(z,t)]J_n[D\hat{H}(w,t)D\Xi(z,t)]^T \\
&= \frac{\partial \Xi}{\partial t}(z,t) + [D\Xi(z,t)]J_n[D\Xi(z,t)]^T\nabla_w\hat{H}(w,t) \\
\dot{w} &= \frac{\partial \Xi}{\partial t}(Z(w,t),t) + J_n\nabla_w\hat{H}(w,t)
\end{aligned}$$

(cf. Meyer & Offin [1]). This is nearly identical to Eqn. (2.2) except for the $\partial\Xi/\partial t$ term. If there is a differentiable function $R : \mathbb{R}^{2n} \times \mathbb{R} \to \mathbb{R}$ such that $\frac{\partial \Xi}{\partial t}(Z(w,t),t) = J_n \nabla_w R(w,t)$, then we do recover Eqn. (2.2) in the new form

$$\dot{w} = J_n \nabla_w \left(R(w,t) + \hat{H}(w,t) \right). \tag{2.4}$$

When a symplectic coordinate change is implemented to turn Eqn. (2.2) into Eqn. (2.4), it is common in the literature to abuse notation and write the new Hamiltonian $R + \hat{H}$ as simply $H(w,t)$ (instead of $H(z,t)$), so that we get $\dot{w} = J_n \nabla_w H(w,t)$ [1].

2.1.1 Rotating Coordinates in the N-Body Problem

The first example of a symplectic coordinate change relevant to this work is a time-dependent rotation in the plane. This is because in our binary asteroid model, we first constrain the motion of the two large primaries that the asteroids orbit. They will be constrained to move in circular tracks according to the solution to Eqn. (1.2) in the case $N = 2$. In order to be able to completely ignore the primaries' motions in simulations, we want to rotate our view along with the motion, so it appears that the primaries are actually fixed.

Such a rotation can be applied to general systems. It is encoded by a time-dependent rotation matrix. For a rotation of constant angular speed ω, the corresponding planar rotation matrix $\mathscr{R}_\omega(t)$ is

$$\mathscr{R}_\omega(t) = \begin{bmatrix} \cos(\omega t) & \sin(\omega t) \\ -\sin(\omega t) & \cos(\omega t) \end{bmatrix}. \tag{2.5}$$

Rotation of the vector (x,y) by the angle ωt is then accomplished by multiplying (x,y) by $R_\omega(t)$.

In the planar N-body problem in particular, we have four Cartesian position vectors $q_i = (x_i, y_i)$ and four momentum vectors $p_i = (p_{x_i}, p_{y_i})$ where $1 \leq i \leq N$. Letting $z = (q_1, \cdots, q_N, p_1, \cdots, p_N) \in \mathbb{R}^{4N}$, we define a transformation $w = (u_1, \cdots, u_N, v_1, \cdots, v_N) = \Xi(z,t)$ by

$$u_i = \mathscr{R}_\omega(t) q_i \text{ and } v_i = \mathscr{R}_\omega(t) p_i,$$

or, as a block-diagonal matrix,

$$w = \Xi(z,t) = \begin{bmatrix} \mathscr{R}_\omega(t) & \cdots & 0 \\ \vdots & \ddots & \vdots \\ 0 & \cdots & \mathscr{R}_\omega(t) \end{bmatrix} z \tag{2.6}$$

where there are $2N$ entries of $\mathscr{R}_\omega(t)$ on the diagonal, one for each of the position and momentum vectors. The Jacobian of Ξ simply drops the rightmost z in Eqn. (2.6), and so it is easy to verify that Ξ satisfies Eqn. (2.3) because $\mathscr{R}_\omega(t)[\mathscr{R}_\omega(t)]^T = I_2$ (i.e., $\mathscr{R}_\omega(t)$ is an orthogonal or unitary matrix).

The time derivative of Ξ can be done term-by-term within the matrix multiplying z. Because $d\mathscr{R}_\omega/dt = \omega J_1 \mathscr{R}_\omega(t)$, we can easily determine the $R(w,t)$ function of Eqn. (2.4) with the observation that

$$\begin{aligned} \nabla_w \left(-\frac{\omega}{2} w^T J_{2N} \begin{bmatrix} J_1 & \cdots & 0 \\ \vdots & \ddots & \vdots \\ 0 & \cdots & J_1 \end{bmatrix} w \right) &= -\omega J_{2N} \begin{bmatrix} J_1 & \cdots & 0 \\ \vdots & \ddots & \vdots \\ 0 & \cdots & J_1 \end{bmatrix} w \\ &= -J_{2N} \begin{bmatrix} \omega J_1 \mathscr{R}_\omega(t) & \cdots & 0 \\ \vdots & \ddots & \vdots \\ 0 & \cdots & \omega J_1 \mathscr{R}_\omega(t) \end{bmatrix} z \\ &= J_{2N}^{-1} \frac{\partial \Xi}{\partial t}(z,t). \end{aligned}$$

Hence, by left multiplying by J_{2N} in the observation, we find $R(w,t)$ is the function

$$R(w,t) = -\frac{\omega}{2} w^T J_{2N} \begin{bmatrix} J_1 & \cdots & 0 \\ \vdots & \ddots & \vdots \\ 0 & \cdots & J_1 \end{bmatrix} w = -\frac{\omega}{2} \begin{bmatrix} -v_1^T & \cdots & -v_N^T & u_1^T & \cdots & u_N^T \end{bmatrix} \begin{bmatrix} J_1 u_1 \\ \vdots \\ J_1 u_N \\ J_1 v_1 \\ \vdots \\ J_1 v_N \end{bmatrix}$$

$$= -\frac{\omega}{2} \left(-\sum_{i=1}^{N} v_i^T J_1 u_i + \sum_{i=1}^{N} u_i^T J_1 v_i \right) = -\frac{\omega}{2} \left(-\sum_{i=1}^{N} u_i^T J_1^T v_i + \sum_{i=1}^{N} u_i^T J_1 v_i \right)$$

$$R(w,t) = -\omega \sum_{i=1}^{N} u_i^T J_1 v_i = -\omega \sum_{i=1}^{N} (u_{x_i} v_{y_i} - u_{y_i} v_{x_i}). \tag{2.7}$$

The addition of this new $R(w,t)$ term into the Hamiltonian is the illustration of the Coriolis effect. As a body away from the origin moves in the rotating reference frame, it experiences an apparent drifting force which appears to make it curve away from the center of rotation. In the inertial frame, however, it is actually the whole system which is rotating underneath the body in question.

2.1.2 Polar-Type Coordinates

Symplectic polar coordinates make use of the well-known polar coordinates formulas:

$$x = r\cos(\theta),\ y = r\sin(\theta), \qquad r = \sqrt{x^2+y^2},\ \theta = \arctan(y/x) \tag{2.8}$$

along with some lesser-known formulas for the corresponding momenta to make the overall transformation symplectic [1]:

$$p_x = p_r \cos(\theta) - \frac{p_\theta}{r}\sin(\theta), \qquad p_y = p_r \sin(\theta) + \frac{p_\theta}{r}\cos(\theta)$$

$$p_r = p_x \cos(\theta) + p_y \sin(\theta) = \frac{x p_x + y p_y}{\sqrt{x^2+y^2}}, \quad p_\theta = -p_x r\sin(\theta) + p_y r\cos(\theta) = x p_y - y p_x. \tag{2.9}$$

In a physical system, the momentum p_θ is the angular momentum of the particle about the origin. This is because in terms of velocities, if the particle has mass m,

$$p_\theta = xp_y - yp_x = mx\dot{y} - my\dot{x} = mr^2\dot{\theta},$$

which corresponds to more well known formulas for this quantity, like in Taylor [2]. Indeed, a celebrated fact of physics is that in "central force" system (e.g., the 2-body problem in the plane), the total angular momentum is conserved. Hence, one of the symmetries we shall exploit in the binary asteroid model will be an introduction of a polar-type symplectic coordinate system where the corresponding p_θ term is constant with respect to time.

2.1.3 Symplectic Scalings

The final family of symplectic coordinate transformations which we discuss here is the family of symplectic scalings. Such scalings allow us to zoom in or out of the origin, and thereby make certain forces dominant or non-dominant. However, they are not strictly symplectic in the sense of Eqn. (2.3); they are actually symplectic "with multiplier," meaning that instead of satisfying Eqn. (2.3), the coordinate transformation $w = \Xi(z)$ satisfies

$$[D\Xi(z)]J_n[D\Xi(z)]^T = \mu J_n \tag{2.10}$$

where $\mu \in \mathbb{R}$ is the so-called multiplier. Once we re-derive the new equation of motion Eqn. (2.4), we find that

$$\dot{w} = \mu J_n \nabla_w \hat{H}(w,t), \tag{2.11}$$

that is, the new Hamiltonian $H = \mu\hat{H}$ is just the old one times the multiplier μ, hence the name.

In a simple system with just one pair of Hamiltonian coordinates (q,p), a symplectic scaling defines a new pair (Q,P) by

$$Q = \delta^\alpha q,\ P = \delta^\beta p, \tag{2.12}$$

where $\delta, \alpha, \beta \in \mathbb{R}$ are fixed parameters, and typically $\delta > 0$ is the desired scale factor. Letting $z = (q, p)$ and $w = (Q, P) = \Xi(z)$ as usual, we find that

$$D\Xi(z) = \begin{bmatrix} \delta^\alpha & 0 \\ 0 & \delta^\beta \end{bmatrix},$$

so that

$$[D\Xi(z)]J_2[D\Xi(z)]^T = \begin{bmatrix} \delta^\alpha & 0 \\ 0 & \delta^\beta \end{bmatrix} \begin{bmatrix} 0 & 1 \\ -1 & 0 \end{bmatrix} \begin{bmatrix} \delta^\alpha & 0 \\ 0 & \delta^\beta \end{bmatrix}^T = \begin{bmatrix} \delta^\alpha & 0 \\ 0 & \delta^\beta \end{bmatrix} \begin{bmatrix} 0 & \delta^\beta \\ -\delta^\alpha & 0 \end{bmatrix}$$
$$= \begin{bmatrix} 0 & \delta^{\alpha+\beta} \\ -\delta^{\alpha+\beta} & 0 \end{bmatrix} = \delta^{\alpha+\beta} J_2.$$

Hence Eqn. (2.12) is indeed symplectic with multiplier $\delta^{\alpha+\beta}$.

More coordinates can be added–the difference is that every copy of Eqn. (2.12) would have all subscripted variables except for δ, which must remain the same in all copies. In such case, we only stipulate that $\alpha_i + \beta_i$ be constant, so that the whole transformation has one multiplier: δ raised to the constant value. Formulating a scaling in this manner allows us to scale different pairs of coordinates differently, although in practice they are all usually scaled the same way.

2.2 Derivations of Hamiltonians

We are now properly prepared to present the Hamiltonians and equations of motion used in our simplified 4-body problem. As a reminder, the principal framework of the model is that we have two large-mass primaries of mass M_1, M_2 and two small-mass asteroids of mass m_1, m_2. We assume that the motions of the primaries are known circular tracks that are not affected by the asteroids' gravity, so that we only have to solve for the motion of the asteroids. For simplicity, we shall also formulate our model in 2-D only; generalizing to a 3-D version is simple but messy.

2.2.1 Binary Asteroid Model

Coordinatize the motion of the primaries by the vectors $\mathfrak{X}_1 = (X_1, Y_1)$ and $\mathfrak{X}_2 = (X_2, Y_2)$. If we reduced the equations of motion (1.1) of the 2-body problem (1.2) into the more familiar version in terms of accelerations and forces, we would find that the primaries must obey

$$\ddot{\mathfrak{X}}_1 = -\frac{M_2(\mathfrak{X}_1 - \mathfrak{X}_2)}{\|\mathfrak{X}_1 - \mathfrak{X}_2\|^3}, \qquad \ddot{\mathfrak{X}}_2 = -\frac{M_1(\mathfrak{X}_2 - \mathfrak{X}_1)}{\|\mathfrak{X}_1 - \mathfrak{X}_2\|^3}. \tag{2.13}$$

A well-known (cf. Taylor [2]) circular solution to this system of differential equations is

$$\begin{aligned} X_1(t) &= -\frac{aM_2}{M}\cos\left(\frac{2\pi t}{P}\right), & Y_1(t) &= -\frac{aM_2}{M}\sin\left(\frac{2\pi t}{P}\right), \\ X_2(t) &= \frac{aM_1}{M}\cos\left(\frac{2\pi t}{P}\right), & Y_2(t) &= \frac{aM_1}{M}\sin\left(\frac{2\pi t}{P}\right), \end{aligned} \tag{2.14}$$

where $a > 0$ is the fixed distance between the primaries, $M = M_1 + M_2$ is their total mass, and $P > 0$ is the period of their motion. These three parameters are related by Kepler's Third Law:

$$\frac{P^2}{a^3} = \frac{4\pi^2}{M}. \tag{2.15}$$

We shall hereafter assume that a and M are arbitrary but fixed, so that P is always uniquely determined.

Now coordinatize the motion of the asteroids by the vectors $q_1 = (x_1, y_1)$ and $q_2 = (x_2, y_2)$. According to any classical mechanics text (cf. Taylor [2]), the kinetic energies of these asteroids are respectively

$$K_1 = \frac{\|p_1\|^2}{2m_1} = \frac{1}{2m_1}(p_{x_1}^2 + p_{y_1}^2), \qquad K_2 = \frac{\|p_2\|^2}{2m_2} = \frac{1}{2m_2}(p_{x_2}^2 + p_{y_1}^2),$$

and if we invoke our assumption that the primaries are immutable sources of gravitational potential, then the total gravitational field experienced by the asteroids is

$$U = -\frac{m_1 m_2}{\|q_1 - q_2\|} - \frac{m_1 M_1}{\|q_1 - \mathfrak{X}_1(t)\|} - \frac{m_2 M_1}{\|q_2 - \mathfrak{X}_1(t)\|} - \frac{m_1 M_2}{\|q_1 - \mathfrak{X}_2(t)\|} - \frac{m_2 M_2}{\|q_2 - \mathfrak{X}_2(t)\|}.$$

The (unrotating) Binary Asteroid Hamiltonian is then simply the total mechanical energy of the system:

$$H_{BA,unrot}(q_i, p_i, t) = K_1 + K_2 + U. \tag{2.16}$$

We note that as written, $H_{BA,unrot}$ is time-dependent due to the presence of $\mathfrak{X}_1(t)$ and $\mathfrak{X}_2(t)$ in the potential energy U.

This time-dependence destroys any hope for preserving conservation of energy in a mathematical sense in this reference frame. However, by utilizing the symplectic rotating coordinates of Section (2.1.1), we can remove the time-dependence and recover conservation. Indeed, to match the motion of the primaries, fix $\omega = 2\pi/P$ and make the transformation of Eqn. (2.6)

$$q_i' = \mathscr{R}_\omega(t) q_i, \; p_i' = \mathscr{R}_\omega(t) p_i.$$

Here primes denote the new coordinates, not derivatives.

Because $\mathscr{R}_\omega(t)$ is an orthogonal matrix, it does not change the lengths of vectors. So the relevant lengths in the kinetic and potential energies are

$$\begin{aligned}
\|p_i\|^2 &= \left\|[\mathscr{R}_\omega(t)]^T p_i'\right\|^2 = \|p_i'\|^2, \\
\|q_1 - q_2\| &= \left\|[\mathscr{R}_\omega(t)]^T q_1' - [\mathscr{R}_\omega(t)]^T q_2'\right\| = \left\|[\mathscr{R}_\omega(t)]^T (q_1' - q_2')\right\| = \|q_1' - q_2'\|, \\
\|q_i - \mathfrak{X}_1(t)\| &= \left\|[\mathscr{R}_\omega(t)]^T q_i' - [\mathscr{R}_\omega(t)]^T (-aM_2/M, 0)\right\| = \left\|[\mathscr{R}_\omega(t)]^T (q_i' + (aM_2/M, 0))\right\| \\
&= \|q_i' + (aM_2/M, 0)\|, \\
\|q_i - \mathfrak{X}_2(t)\| &= \left\|[\mathscr{R}_\omega(t)]^T q_i' - [\mathscr{R}_\omega(t)]^T (aM_1/M, 0)\right\| = \left\|[\mathscr{R}_\omega(t)]^T (q_i' - (aM_1/M, 0))\right\| \\
&= \|q_i' - (aM_1/M, 0)\|.
\end{aligned}$$

The substituted Hamiltonian $\hat{H}_{BA,unrot}$ is therefore

$$\begin{aligned}
\hat{H}_{BA,unrot}(q_i', p_i', t) = \frac{\|p_1'\|^2}{2m_1} + \frac{\|p_2'\|^2}{2m_2} - \frac{m_1 m_2}{\|q_1' - q_2'\|} - \frac{m_1 M_1}{\|q_1' + (aM_2/M, 0)\|} - \frac{m_2 M_1}{\|q_2' + (aM_2/M, 0)\|} \\
- \frac{m_1 M_2}{\|q_1' - (aM_1/M, 0)\|} - \frac{m_2 M_2}{\|q_2' - (aM_1/M, 0)\|}.
\end{aligned}$$

Since we have the remainder function $R(q_i', p_i', t)$ from Eqn. (2.7), we conclude that the rotating Binary Asteroid Hamiltonian is $R + \hat{H}$:

$$H_{BA}(q_i', p_i') = \frac{\|p_1'\|^2}{2m_1} + \frac{\|p_2'\|^2}{2m_2} - \frac{2\pi}{P}\left((q_1')^T J_1 p_1' + (q_2')^T J_1 p_2'\right) - \frac{m_1 m_2}{\|q_1' - q_2'\|} - \frac{m_1 M_1}{\|q_1' + (aM_2/M, 0)\|} - \frac{m_2 M_1}{\|q_2' + (aM_2/M, 0)\|} - \frac{m_1 M_2}{\|q_1' - (aM_1/M, 0)\|} - \frac{m_2 M_2}{\|q_2' - (aM_1/M, 0)\|}. \tag{2.17}$$

To keep things clean, we will abuse notation slightly and drop the primes on all coordinates. Upon doing so, we obtain the form of H_{BA} which we use in the analysis sections:

$$H_{BA} = \frac{1}{2m_1}\left(p_{x_1}^2 + p_{y_1}^2\right) + \frac{1}{2m_2}\left(p_{x_2}^2 + p_{y_2}^2\right) - \frac{2\pi}{P}\left(x_1 p_{y_1} - y_1 p_{x_1}\right) - \frac{2\pi}{P}\left(x_2 p_{y_2} - y_2 p_{x_2}\right) - \frac{m_1 m_2}{\sqrt{(x_1 - x_2)^2 + (y_1 - y_2)^2}} - \frac{m_1 M_1}{\sqrt{(x_1 + aM_2/M)^2 + y_1^2}} - \frac{m_2 M_1}{\sqrt{(x_2 + aM_2/M)^2 + y_2^2}} - \frac{m_1 M_2}{\sqrt{(x_1 - aM_1/M)^2 + y_1^2}} - \frac{m_2 M_2}{\sqrt{(x_2 - aM_1/M)^2 + y_2^2}}. \tag{2.18}$$

Notice that H_{BA} is time-independent! Therefore we can recover conservation of energy, because by the Chain Rule and the equations of motion (1.1),

$$\begin{aligned}\frac{dH_{BA}}{dt} &= \frac{\partial H_{BA}}{\partial t} + \sum_{i=1}^{2}\left(\frac{\partial H_{BA}}{\partial x_i}\dot{x_i} + \frac{\partial H_{BA}}{\partial y_i}\dot{y_i} + \frac{\partial H_{BA}}{\partial p_{x_i}}\dot{p_{x_i}} + \frac{\partial H_{BA}}{\partial p_{y_i}}\dot{p_{y_i}}\right) \\ &= \sum_{i=1}^{2}\left(\frac{\partial H_{BA}}{\partial x_i}\frac{\partial H_{BA}}{\partial p_{x_i}} + \frac{\partial H_{BA}}{\partial y_i}\frac{\partial H_{BA}}{\partial p_{y_i}} - \frac{\partial H_{BA}}{\partial p_{x_i}}\frac{\partial H_{BA}}{\partial x_i} - \frac{\partial H_{BA}}{\partial p_{y_i}}\frac{\partial H_{BA}}{\partial y_i}\right) \\ &= 0.\end{aligned}$$

So, for any flow $q_i = q_i(t)$, $p_i = p_i(t)$ subject to (1.1), we have the conservation law

$$H_{BA}(q_i(t), p_i(t)) = \text{constant}. \tag{2.19}$$

This "first integral" is important to the invocation of the continuation results in Section 2.3.

2.2.2 Center-of-Mass Reduction

Equation (2.18), while qualitatively simple, is still quite unwieldy when we translate down to the equations of motion. Indeed, there are eight variables, and therefore eight differential equations to

solve. To further reduce this complexity, we shall introduce a barycentric symmetry.

Ordinarily, a physical system like the N-body problem exhibits conservation of momentum due to Newton's Third Law. Because of the definition of the momentum, this conservation means that the center-of-mass (COM) moves with constant velocity. Since we are free to examine physical systems in different inertial reference frames, we can safely ignore this COM motion, and simply posit that it remains fixed at the origin–a barycentric coordinate system.

However, in the Binary Asteroid Hamiltonian H_{BA}, the motion of the primaries means that we (a priori) remove the conservation of momentum, because we aren't allowing the primaries to experience an "equal and opposite reaction" from the asteroids' gravity. So in general, we do not get barycentric symmetry in the equations of motion for (2.18).

Despite this, there is a family of mass configurations for which the symmetry is restored. Suppose we have equal-masses in the pairs, that is,

$$M_1 = M_2 = \frac{M}{2} \text{ and } m_1 = m_2 =: m. \tag{2.20}$$

The Binary Asteroid Hamiltonian becomes

$$\begin{aligned} H_{BA} = &\frac{1}{2m}\left(p_{x_1}^2 + p_{y_1}^2\right) + \frac{1}{2m}\left(p_{x_2}^2 + p_{y_2}^2\right) - \frac{2\pi}{P}\left(x_1 p_{y_1} - y_1 p_{x_1}\right) - \frac{2\pi}{P}\left(x_2 p_{y_2} - y_2 p_{x_2}\right) \\ &- \frac{m^2}{\sqrt{(x_1-x_2)^2+(y_1-y_2)^2}} - \frac{mM/2}{\sqrt{(x_1+a/2)^2+y_1^2}} - \frac{mM/2}{\sqrt{(x_2+a/2)^2+y_2^2}} \\ &- \frac{mM/2}{\sqrt{(x_1-a/2)^2+y_1^2}} - \frac{mM/2}{\sqrt{(x_2-a/2)^2+y_2^2}}. \end{aligned} \tag{2.21}$$

Additionally, the two pairs of bodies have pair barycenters

$$\begin{aligned} \mathfrak{x}_{COM} &= \frac{M_1\mathfrak{x}_1 + M_2\mathfrak{x}_2}{M_1+M_2} = \frac{\frac{M}{2}(-aM_2/M,0) + \frac{M}{2}(aM_1/M,0)}{M} = \frac{(-a/2,0)+(a/2,0)}{2} = (0,0) \\ q_{COM} &= \frac{m_1 q_1 + m_2 q_2}{m_1+m_2} = \frac{mq_1+mq_2}{2m} = \frac{q_1+q_2}{2}. \end{aligned}$$

We would like to stipulate that $q_{COM} = \mathfrak{x}_{COM} = (0,0)$, so that the whole system barycenter is at the origin. To do so, we shall investigate a barycentric symplectic change of coordinates.

Consider the matrix

$$\mathscr{M} = \frac{1}{2}\begin{bmatrix} 1 & 0 & -1 & 0 \\ 0 & 1 & 0 & -1 \\ 1 & 0 & 1 & 0 \\ 0 & 1 & 0 & 1 \end{bmatrix}.$$

We shall change coordinates from (x_1, y_1, x_2, y_2) to (x, y, α, β) by the equations

$$\begin{bmatrix} x & y & \alpha & \beta \end{bmatrix}^T = \mathscr{M}\begin{bmatrix} x_1 & y_1 & x_2 & y_2 \end{bmatrix}^T, \quad \begin{bmatrix} p_x & p_y & p_\alpha & p_\beta \end{bmatrix}^T = (\mathscr{M}^{-1})^T\begin{bmatrix} p_{x_1} & p_{y_1} & p_{x_2} & p_{y_2} \end{bmatrix}^T$$

or, more explicitly,

$$\begin{aligned} x &= \frac{x_1 - x_2}{2}, & y &= \frac{y_1 - y_2}{2}, & \alpha &= \frac{x_1 + x_2}{2}, & \beta &= \frac{y_1 + y_2}{2}, \\ p_x &= p_{x_1} - p_{x_2}, & p_y &= p_{y_1} - p_{y_2}, & p_\alpha &= p_{x_1} + p_{x_2}, & p_\beta &= p_{y_1} + p_{y_2}. \end{aligned} \tag{2.22}$$

The coordinates x and y represent (half) the relative position between the two asteroids. The coordinates α and β, called the COM coordinates, represent the components of the asteroids' barycenter. The Jacobian of this transformation is

$$D\Xi(z) = \begin{bmatrix} \mathscr{M} & 0 \\ 0 & (\mathscr{M}^{-1})^T \end{bmatrix} = \begin{bmatrix} \mathscr{M} & 0 \\ 0 & 2\mathscr{M} \end{bmatrix}$$

and it is symplectic inasmuch as

$$\begin{aligned} [D\Xi(z)]J_4[D\Xi(z)]^T &= \begin{bmatrix} \mathscr{M} & 0 \\ 0 & (\mathscr{M}^{-1})^T \end{bmatrix}\begin{bmatrix} 0 & I_4 \\ -I_4 & 0 \end{bmatrix}\begin{bmatrix} \mathscr{M}^T & 0 \\ 0 & \mathscr{M}^{-1} \end{bmatrix} \\ &= \begin{bmatrix} \mathscr{M} & 0 \\ 0 & (\mathscr{M}^{-1})^T \end{bmatrix}\begin{bmatrix} 0 & \mathscr{M}^{-1} \\ -\mathscr{M}^T & 0 \end{bmatrix} = \begin{bmatrix} 0 & I_4 \\ -I_4 & 0 \end{bmatrix} \\ &= J_4. \end{aligned}$$

The new Hamiltonian is

$$\begin{aligned} H_{BA,COM} = \frac{1}{4m}\left(p_x^2+p_y^2\right)+\frac{1}{4m}\left(p_\alpha^2+p_\beta^2\right)-\frac{2\pi}{P}\left(xp_y-yp_x+\alpha p_\beta-\beta p_\alpha\right) \\ -\frac{m^2}{2\sqrt{x^2+y^2}}-\frac{mM/2}{\sqrt{(x+\alpha+\frac{a}{2})^2+(y+\beta)^2}}-\frac{mM/2}{\sqrt{(x-\alpha-\frac{a}{2})^2+(y-\beta)^2}} \\ -\frac{mM/2}{\sqrt{(x+\alpha-\frac{a}{2})^2+(y+\beta)^2}}-\frac{mM/2}{\sqrt{(x-\alpha+\frac{a}{2})^2+(y-\beta)^2}}. \end{aligned} \tag{2.23}$$

In order to satisfy our stipulation that $q_{COM} = \mathfrak{X}_{COM} = (0,0)$, we want to force $\alpha = \beta = 0$ (and, as it turns out, $p_\alpha = p_\beta = 0$).

To determine whether this is possible to force, consider the equations of motion (1.1) for the COM coordinates under the Hamiltonian (2.23):

$$\begin{aligned} \dot{\alpha} &= \frac{\partial H_{BA,COM}}{\partial p_\alpha} = \frac{p_\alpha}{2m}+\frac{2\pi\beta}{P}, \\ \dot{\beta} &= \frac{\partial H_{BA,COM}}{\partial p_\beta} = \frac{p_\beta}{2m}-\frac{2\pi\alpha}{P}, \\ \dot{p}_\alpha &= -\frac{\partial H_{BA,COM}}{\partial \alpha} = \frac{2\pi p_\beta}{P}-\frac{mM(x+\alpha+a/2)/2}{((x+\alpha+\frac{a}{2})^2+(y+\beta)^2)^{3/2}}+\frac{mM(x-\alpha-a/2)/2}{((x-\alpha-\frac{a}{2})^2+(y-\beta)^2)^{3/2}} \\ &\quad -\frac{mM(x+\alpha-a/2)/2}{((x+\alpha-\frac{a}{2})^2+(y+\beta)^2)^{3/2}}+\frac{mM(x-\alpha+a/2)/2}{((x-\alpha+\frac{a}{2})^2+(y-\beta)^2)^{3/2}} \\ \dot{p}_\beta &= -\frac{\partial H_{BA,COM}}{\partial \beta} = -\frac{2\pi p_\alpha}{P}-\frac{mM(y+\beta)/2}{((x+\alpha+\frac{a}{2})^2+(y+\beta)^2)^{3/2}}+\frac{mM(y-\beta)/2}{((x-\alpha-\frac{a}{2})^2+(y-\beta)^2)^{3/2}}, \\ &\quad -\frac{mM(y+\beta)/2}{((x+\alpha-\frac{a}{2})^2+(y+\beta)^2)^{3/2}}+\frac{mM(y-\beta)/2}{((x-\alpha+\frac{a}{2})^2+(y-\beta)^2)^{3/2}}. \end{aligned} \tag{2.24}$$

Substituting the guess $\alpha = \beta = p_\alpha = p_\beta = 0$, these become

$$\begin{aligned}
\dot{\alpha} &= 0, \\
\dot{\beta} &= 0, \\
\dot{p}_\alpha &= 0 - \frac{mM(x+a/2)/2}{((x+\frac{a}{2})^2+y^2)^{3/2}} + \frac{mM(x-a/2)/2}{((x-\frac{a}{2})^2+y^2)^{3/2}} - \frac{mM(x-a/2)/2}{((x-\frac{a}{2})^2+y^2)^{3/2}} + \frac{mM(x+a/2)/2}{((x+\frac{a}{2})^2+y^2)^{3/2}} \\
&= 0, \\
\dot{p}_\beta &= 0 - \frac{mMy/2}{((x+\frac{a}{2})^2+y^2)^{3/2}} + \frac{mMy/2}{((x-\frac{a}{2})^2+y^2)^{3/2}} - \frac{mMy/2}{((x-\frac{a}{2})^2+y^2)^{3/2}} + \frac{mMy/2}{((x+\frac{a}{2})^2+y^2)^{3/2}} \\
&= 0.
\end{aligned}$$

Thus, forcing $\alpha = \beta = p_\alpha = p_\beta = 0$ is consistent with the equations of motion.

Now consider the remaining four equations of motion. The x, y equations associated with (2.23) are

$$\begin{aligned}
\dot{x} &= \frac{\partial H_{BA,COM}}{\partial p_x} = \frac{p_x}{2m} + \frac{2\pi y}{P}, \\
\dot{y} &= \frac{\partial H_{BA,COM}}{\partial p_y} = \frac{p_y}{2m} - \frac{2\pi x}{P}, \\
\dot{p}_x &= -\frac{\partial H_{BA,COM}}{\partial x} = \frac{2\pi p_y}{P} - \frac{mM(x+\alpha+a/2)/2}{((x+\alpha+\frac{a}{2})^2+(y+\beta)^2)^{3/2}} - \frac{mM(x-\alpha-a/2)/2}{((x-\alpha-\frac{a}{2})^2+(y-\beta)^2)^{3/2}} \\
&\quad - \frac{mM(x+\alpha-a/2)/2}{((x+\alpha-\frac{a}{2})^2+(y+\beta)^2)^{3/2}} - \frac{mM(x-\alpha+a/2)/2}{((x-\alpha+\frac{a}{2})^2+(y-\beta)^2)^{3/2}} - \frac{m^2 x/2}{(x^2+y^2)^{3/2}} \\
\dot{p}_y &= -\frac{\partial H_{BA,COM}}{\partial y} = -\frac{2\pi p_x}{P} - \frac{mM(y+\beta)/2}{((x+\alpha+\frac{a}{2})^2+(y+\beta)^2)^{3/2}} - \frac{mM(y-\beta)/2}{((x-\alpha-\frac{a}{2})^2+(y-\beta)^2)^{3/2}} \\
&\quad - \frac{mM(y+\beta)/2}{((x+\alpha-\frac{a}{2})^2+(y+\beta)^2)^{3/2}} - \frac{mM(y-\beta)/2}{((x-\alpha+\frac{a}{2})^2+(y-\beta)^2)^{3/2}} - \frac{m^2 y/2}{(x^2+y^2)^{3/2}}.
\end{aligned} \tag{2.25}$$

Substituting the $\alpha = \beta = p_\alpha = p_\beta = 0$ guess into Eqn. (2.25) gives

$$\begin{aligned}
\dot{x} &= \frac{p_x}{2m} + \frac{2\pi y}{P}, \\
\dot{y} &= \frac{p_y}{2m} - \frac{2\pi x}{P}, \\
\dot{p}_x &= \frac{2\pi p_y}{P} - \frac{mM(x-a/2)}{((x-\frac{a}{2})^2+y^2)^{3/2}} - \frac{mM(x+a/2)}{((x+\frac{a}{2})^2+y^2)^{3/2}} - \frac{m^2 x}{2(x^2+y^2)^{3/2}} \\
\dot{p}_y &= -\frac{2\pi p_x}{P} - \frac{mMy}{((x-\frac{a}{2})^2+y^2)^{3/2}} - \frac{mMy}{((x+\frac{a}{2})^2+y^2)^{3/2}} - \frac{m^2 y}{2(x^2+y^2)^{3/2}}.
\end{aligned} \tag{2.26}$$

Fortunately, the equations (2.26) are Hamiltonian, in the form of Eqn. (1.1)! The reduced Hamiltonian is

$$\begin{aligned}
H_{xy}(x,y,p_x,p_y) = \frac{1}{4m}\left(p_x^2+p_y^2\right) - \frac{2\pi}{P}\left(xp_y - yp_x\right) - \frac{m^2}{2\sqrt{x^2+y^2}} \\
- \frac{mM}{\sqrt{(x+a/2)^2+y^2}} - \frac{mM}{\sqrt{(x-a/2)^2+y^2}}.
\end{aligned} \tag{2.27}$$

The punchline here is that we can solve the Binary Asteroid Hamiltonian (2.21) under the equal-pair mass condition (2.20) by simply solving Eqn. (2.26) for x, y, p_x, p_y. Physically, the symmetry being exploited is the fact that when $\alpha = \beta = p_\alpha = p_\beta = 0$, the original coordinates have $x_1 = -x_2$ and $y_1 = -y_2$. That is, the motion of one of the asteroids is perfectly reflected by the other.

Remarkably, the form of the Hamiltonian (2.27) is nearly identical to the circular restricted 4-body problem presented in Llibre et al. [8]. This means that many of the dynamics are the same. However, the physical interpretation is different. Where their problem models the motion of a massless particle moving in the gravity of three primaries in a line, our problem is an encoding of the motion of two positive mass particles.

2.3 Continuation Methods

As we utilize symplectic scalings to make specific behaviors dominant, we need to take care to ensure the perturbations of the Hamiltonian that we make do not destroy the underlying dynamics. The dynamical features we are interested in are relative equilibria and periodic orbits. Certain theorems in general dynamical systems theory can be applied to ensure these features persist or "continue" through the perturbation.

In this section, we detour toward general dynamical systems theory in order to give the proper statements of the relevant theorems. We will consider an n-dimensional autonomous dynamical system given by

$$\dot{z} = f(z, \nu), \tag{2.28}$$

where $z(t) \in \mathbb{R}^n$ and $\nu \in \mathbb{R}^k$ is a vector of parameters which perturb the dynamical system. We also assume that f is a smooth (infinitely differentiable) function in both parameters.

2.3.1 Periodic Orbits

The majority of our results pertain to the determination of periodic solutions to the equations of motion of the Binary Asteroid Hamiltonian (2.18). In our analyses, we encounter simplified systems of the form (2.28) where ν is a scalar quantity, namely, the scale factor from a symplectic scaling. Certain values of this parameter yield versions of the equations of motion where periodic solutions are easy to identify and write down. However, as we change ν, the previously non-dominant gravitational forces will begin to affect the dynamics, thereby changing the geometry of the solutions.

In the general language of Eqn. (2.28), suppose for a fixed ν_0 and an initial condition z_0, we have a periodic solution $z(t)$ of the system with minimal period $T > 0$, that is, $z(t+T) = z(t)$ for all t. We shall keep track of the initial condition and parameter vector by writing $z(t) = \phi(t, z_0, \nu_0)$.

A continuation of this periodic solution is a pair of functions $\zeta(\nu)$, $\tau(\nu)$ defined near ν' such that $\zeta(\nu_0) = z_0$, $\tau(\nu_0) = T$, and the function $\phi(t, \zeta(\nu), \nu)$ is a periodic solution of (2.28) with initial condition $\zeta(\nu)$ of minimal period $\tau(\nu)$.

To show the existence of a continuation, one must analyze the "monodromy matrix" of the original periodic orbit $\phi(t, z_0, \nu_0)$. This is the matrix $D_\zeta \phi(T, z_0, \nu_0)$, where D_ζ denotes the Jacobian of the solution with respect to the initial condition ζ, and we evaluate it at $t = T$ (the period) and $\zeta = z_0$. The eigenvalues of the monodromy matrix are called the (characteristic) multipliers of the periodic solution. It can be shown that $+1$ is always a multiplier with eigenvector $f(z_0, \nu_0)$. Furthermore, if the system (2.28) is Hamiltonian, then $+1$ has algebraic multiplicity at least two (cf. Meyer & Offin [1]).

When the algebraic multiplicity of $+1$ is exactly one (two if Hamiltonian), the periodic orbit $\phi(t, z_0, \nu_0)$ is said to be elementary. The continuation theorem relevant to this work is then the simple statement that "all elementary periodic orbits can be continued." A more formal statement is the following:

Theorem 1. ***(Continuation of Periodic Orbits)*** *Let $\phi(t, z_0, \nu_0)$ be an elementary periodic solution of the dynamical system Eqn.* (2.28) *with $\nu = \nu_0$. Then there exists a continuation $\zeta(\nu), \tau(\nu)$ such that the function $z(t) = \phi(t, \zeta(\nu), \nu)$ is a $\tau(\nu)$-periodic solution of the same system with ν now near to but away from ν_0.*

Proof. See Proposition 9.1.1 in Meyer & Offin [1]. □

2.3.2 Relative Equilibria and the Lyapunov Center Theorem

The other portion of our results pertain to the existence and spectra of relative equilibria. Given a fixed ν, an equilibrium point for the system (2.28) is a configuration $\xi \in \mathbb{R}^n$ so that $f(\xi, \nu) = 0$. Such configurations are of interest because $z(t) = \xi$ is a solution of the dynamical system. In the

N-body problem (1.2), there are no equilibria according to this definition, however, if we adopt the rotating reference frame of Section 2.1.1, then the new Hamiltonian does induce equilibria. These equilibria are unchanging configurations in the rotating frame; in an inertial reference frame, they move according to the rotation. For this reason, the equilibria of, say, the Binary Asteroid Hamiltonian (2.18) are called "relative" equilibria. We shall investigate such configurations in Chapter 4.

Near an equilibrium point, we can expect the dynamics to be similar to those induced by a linear f, namely, the Jacobian $D_z f(\xi, \nu)$ evaluated at the equilibrium. Because the solution to the linear system $\dot{z} = Az$ is the matrix exponential $z(t) = e^{tA} z_0$, the dynamics of the matrix A are determined by its eigenvalues λ and what happens when we take the exponential e^{λ}. Therefore, if ξ is an equilibrium for Eqn. (2.28), we are interested in the eigenvalues of $D_z f(\xi, \nu)$, called the (characteristic) exponents of the equilibrium. If all of the exponents are nonzero, then $D_z f(\xi, \nu)$ is invertible, and we call ξ an elementary equilibrium.

Figure 1.1 displays the most prominent examples of elementary relative equilibria in celestial mechanics, the celebrated Lagrange points of the CR3BP, labeled L_1 through L_5. The first three points lie on the line defined by the primaries, and the points L_4 and L_5 form equilateral triangles. In our model, we find remnants of these Lagrange points due to the similarities to the CR3BP.

One reason for studying elementary relative equilibria is that there is the possibility of periodic orbits around such points, depending on the exponents. These are called Lyapunov or central orbits, after the following theorem:

Theorem 2. ***(Lyapunov Center Theorem)*** *Suppose the system* (2.3) *is Hamiltonian with an equilibrium point ξ whose exponents are $\pm i\omega, \lambda_3, \cdots, \lambda_m$, where ω is nonzero real. If $\lambda_j / i\omega$ is never an integer for any $3 \leq j \leq m$, then there exists a family of periodic orbits emanating from the equilibrium point. When approaching ξ along this family, the periods tend to $2\pi/\omega$ and the non-one multipliers of the solutions tend to* $\exp(2\pi\lambda_j/\omega)$.

Proof. See Theorem 9.2.1 in Meyer & Offin [1]. The proof makes use of Theorem 1. □

The Lagrange points of the CR3BP are examples of Lyapunov centers. Figure 2.1 shows an example of the emanating orbits about them in the case of the Earth-Moon-Satellite three-body system in rotating coordinates.

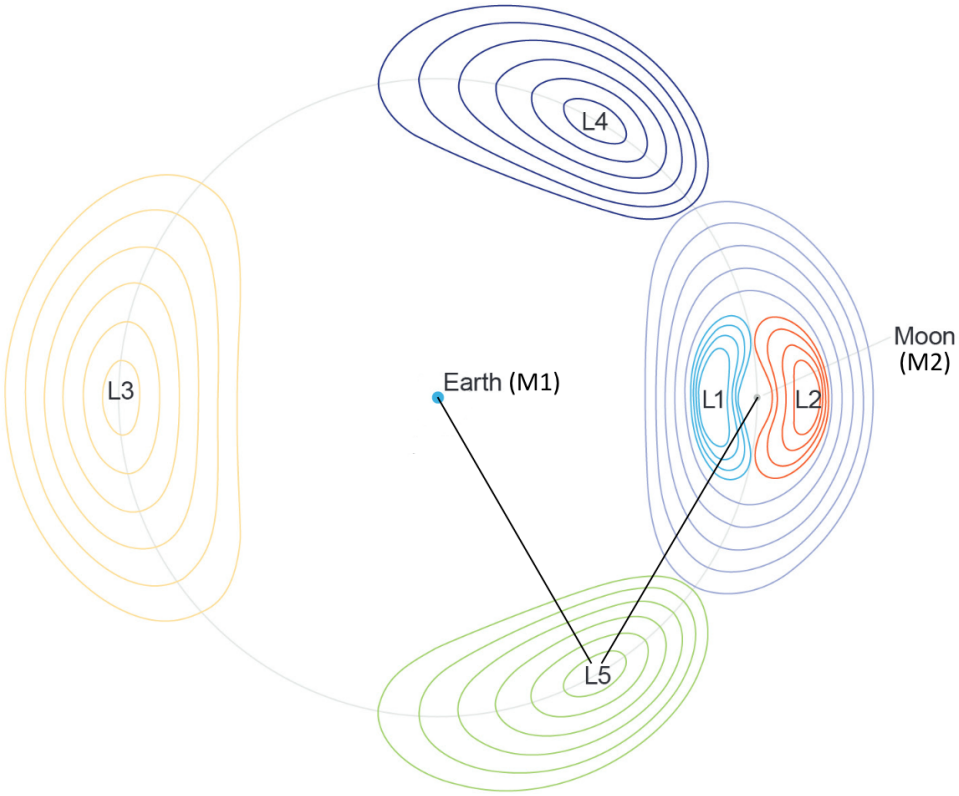

Figure 2.1 Diagram showing the Lyapunov central orbits about the Lagrange points of the three-body problem defined by the Earth and Moon. The black lines connecting the Earth and Moon to L_5 are of equal length, forming an equilateral triangle. Figure adapted from Pollock IV & Vedda [11].

Chapter 3

Numerical Investigations

Many of the analytical results in this work were initially motivated by similar results in other problems like the CR3BP, the collinear restricted 4-body problem of Llibre et al. [8], or the equilateral triangle restricted 4-body problem of Alvarez-Ramírez [9], as well as numerical studies of our model equations of motion. This chapter compiles a list of graphs from the results of the numerical studies. These graphs will be cited as we present the analytical results.

3.1 Software Methods

All graphs were generated using the `ode45` differential equation solver in MATLAB. The solver implements a corrective explicit Runge-Kutta type method for initial-value problems of the form $\dot{z} = f(z,t)$. To utilize this routine, we derived the equations of motion (1.1) for each relevant Hamiltonian (e.g., Eqns. (2.18), (2.23), and (2.27)), taking the derivatives using the `D` function in Mathematica.

For example, Eqns. (2.24) and (2.25) are the equations associated with the COM Binary Asteroid Hamiltonian (2.23), whereas Eqn. (2.26) are the equations associated with H_{xy} (2.27). We omit the equations for the Cartesian Binary Asteroid Hamiltonian (2.18) due to their length and complexity.

In choosing initial conditions, we pre-selected baseline values of the positions and momenta, and then perturbed the momenta from those presets, running new simulations for each perturbed value of momentum. The presets shown here were derived from the relative equilibria and periodic solutions obtained in the subsequent analyses. The action of momentum perturbation served to create a "shooting method" for finding interesting dynamics, because the initial position would remain fixed while we edited the initial velocity.

Since we are more interested in the geometry of the solutions rather than the actual time-dependencies of the different coordinates, we present coordinate-versus-coordinate (i.e., x vs. y, etc.) graphs instead of coordinate-versus-time graphs. The former is much more illuminating than the latter for a few reasons, one being that it is easier to see whether an orbit is periodic–it must be a closed curve.

3.2 Hill, Comet, and Intermediate Orbits

The simplest illustrations of the "shooting method" in action are the Hill and comet type orbits, explored in more detail in Chapter 5. The Hill orbits couple each asteroid to each primary (for example, the left asteroid m_1 goes to the left primary M_1, etc.), making that primary's gravity the dominant force on the respective asteroid. By contrast, the comet orbits place both asteroids far enough away from the primaries that their combined gravity approximately equals that of a single massive particle.

There is also the possibility of an intermediate class of orbit between the Hill and Comet cases. Here, the asteroids are not bound to a single primary, but they are also not orbiting far away. The asteroids could switch which primary they are near. We do not have any analytical results about the intermediate orbits; our numerical simulations suggest that periodic intermediate orbits exist but are extremely unstable. Figure 3.1 shows some examples of these simulations, as well as examples

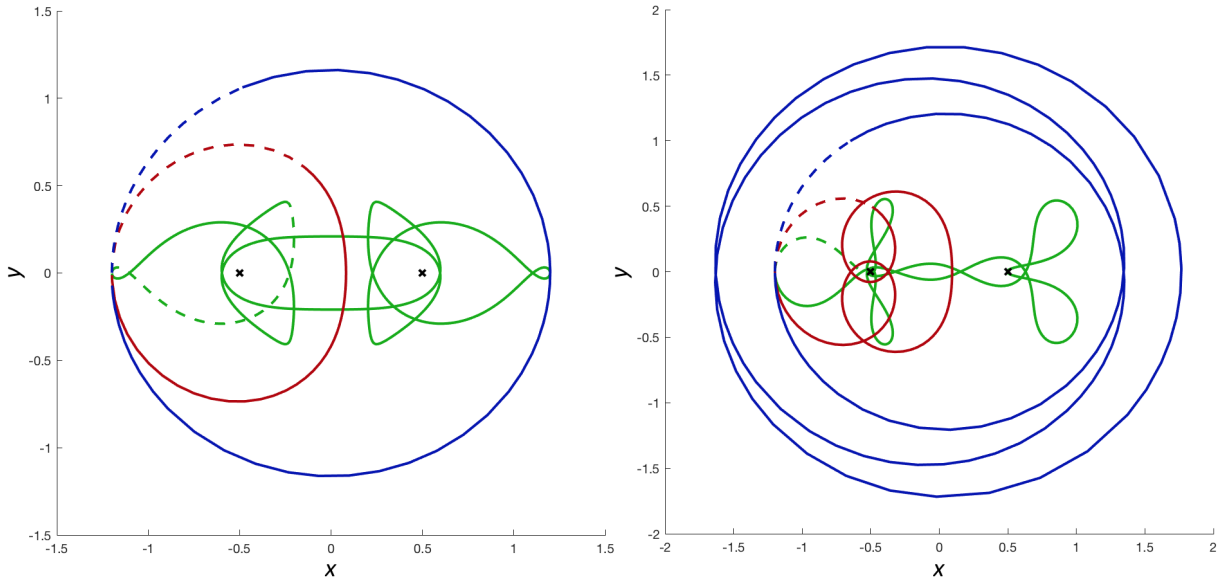

Figure 3.1 Depiction of Hill (red), comet (blue), and intermediate (green) orbits in the Binary Asteroid problem (2.18). The primaries are marked as black x's. In both plots, only one asteroid track is shown for clarity. The equal-pair condition (2.20) applies here, hence the hidden asteroid orbits the same displayed track, but reflected about the line $x = 0$. Each orbit was generated by placing the asteroids near the L_2 and L_3 Lagrange points defined by the primaries, then using the shooting method to alter the velocity to taste. The dotted parts of the tracks display the initial trajectories.

of Hill and comet orbits. This figure also demonstrates that these simple orbit classes need not be circular, elliptical, or even symmetric about the vertical axis.

Despite the fact that the Hill and comet orbits need not exhibit elliptic structure, that form is the simplest kind of periodic behavior. In the analysis therefore, we prove the existence of near-circular periodic Hills and comets. The idea is that as the asteroids get closer to (resp. farther from) the primary(-ies), the gravitational field resembles that of a rotating 2-body problem, which has known circular orbits. This can be understood concretely by way of Theorem 1. As such, Fig. 3.2 displays this continuation process. The near-circular Hill orbits appear to emanate from the primaries, while the comet orbits appear to "emanate" from infinity.

We emphasize that although Figures 3.1 and 3.2 made use of the equal-pair condition (2.20),

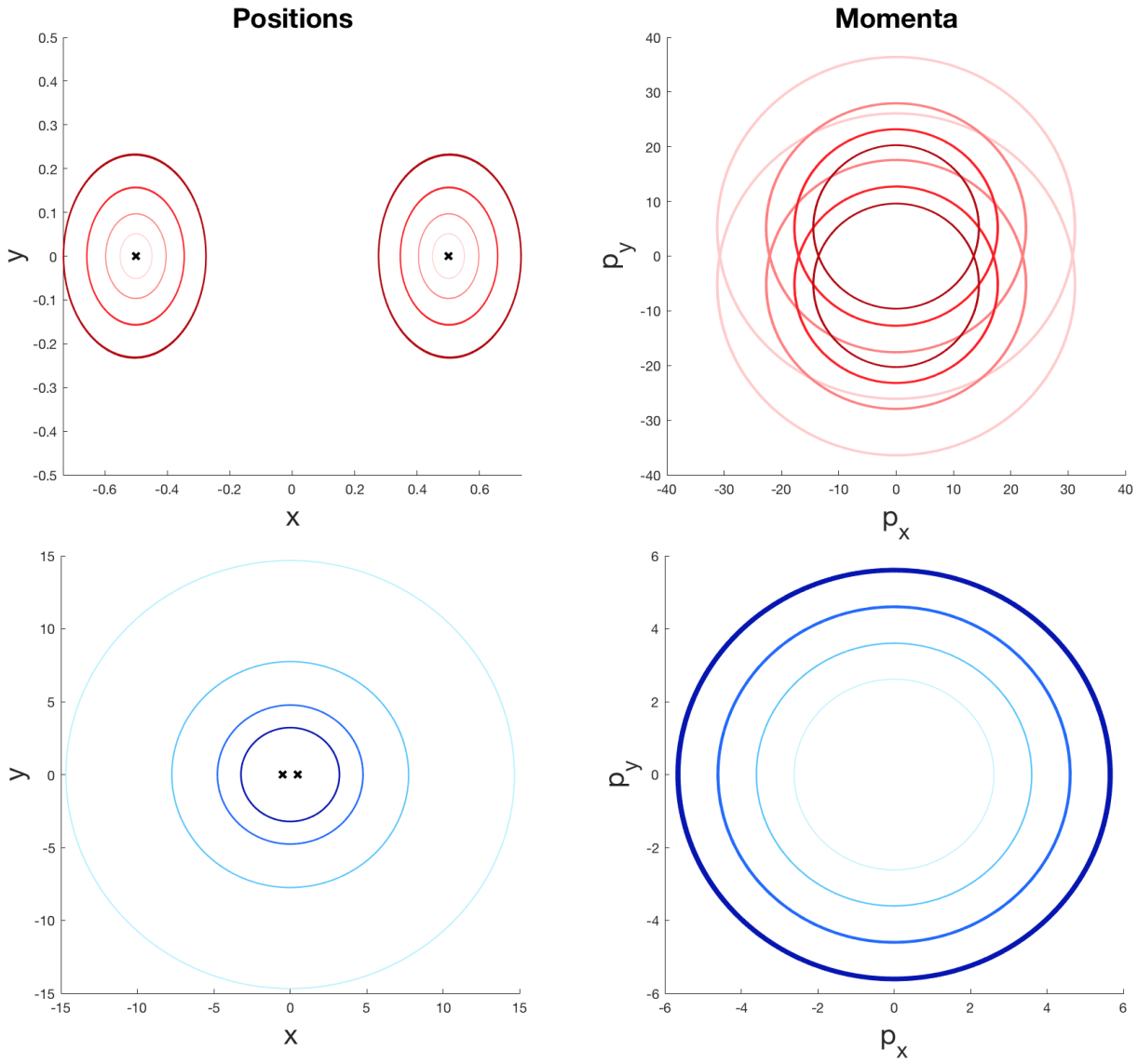

Figure 3.2 An example of how Theorem 1 applies to generate near-circular Hill orbits (top) and comet orbits (bottom) under the equal-pair condition (2.20). The primaries are marked as black x's. Both asteroids' tracks are shown, with matching colors indicating the same initial conditions. Note that in the comet orbits, the asteroids orbit on the same track.

there is evidence that these Hill and comet orbits persist even in the unequal-mass cases. Indeed, we show in Chapter 5 that near-circular periodic comet orbits exist for any physically reasonable selection of the four masses M_1, M_2, m_1, m_2. However, the evidence for near-circular periodic Hill

orbits of arbitrary mass is purely numerical. Figure 3.3 demonstrates what happens to the darkest Hill orbit in Fig. 3.2 if we perturb the primaries' masses to be different. The pure circularity is lost, so these orbits may only be quasi-periodic.

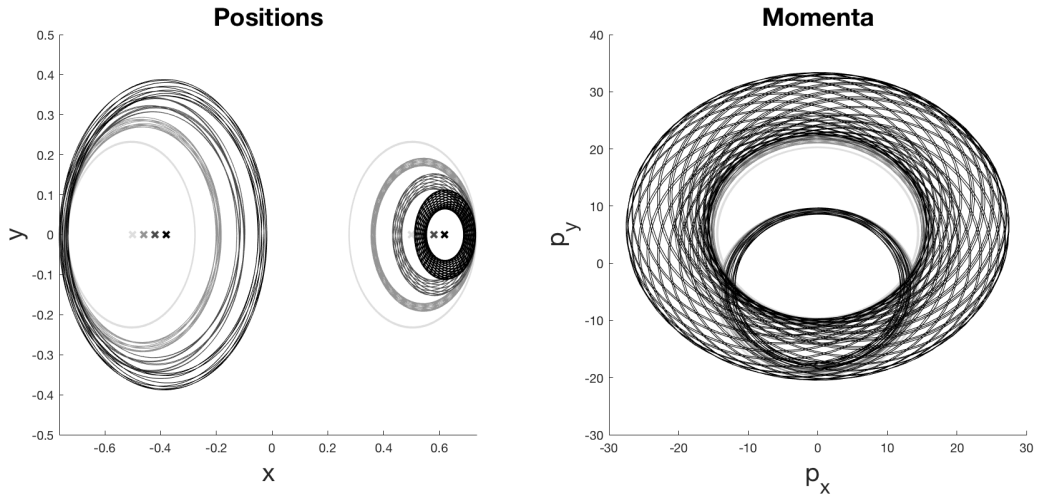

Figure 3.3 Simulations of Hill orbits using the same initial conditions as the darkest orbit in Fig. 3.2, but with different primary masses M_1 and M_2. The primaries are marked with shaded x's according to the corresponding simulation. Note that the primaries are not moving in time–the act of changing the masses affects where the origin is placed relative to the primaries.

There is one more phenomenon to consider with the Hill orbits. In Chapter 5 we prove that the near-circular Hills are characterized by the asteroids' angular momenta p_θ about the respective primaries. Numerical simulation suggests that the positive-momentum and negative-momentum orbits have varying stability. This is likely because the one causes the asteroids to rotate in the same direction as the reference frame, whereas the other causes them rotate opposite that direction. Figure 3.4 displays a more extreme version of the Hill continuation in Fig. 3.2, chosen to illustrate the differences between the positive and negative angular momentum orbits.

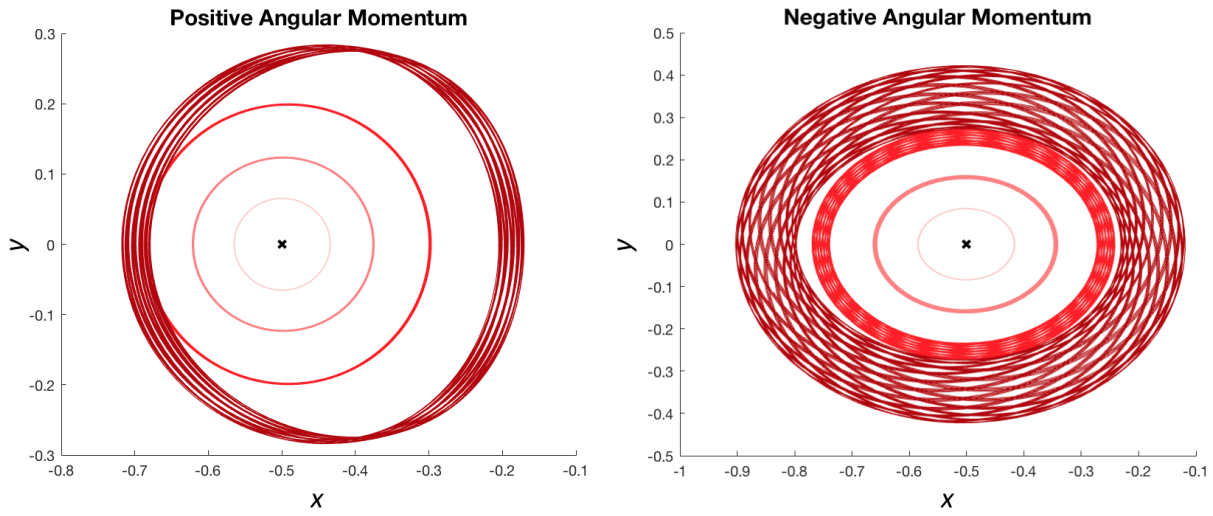

Figure 3.4 Continuation of near-circular Hill orbits to the dark-red extremes which illustrate the distinct geometries of positive and negative angular momentum orbits. Only one asteroid orbit is shown.

3.3 Orbits about Equilibria

The periodic Lyapunov center orbits mentioned Section 2.3.2 exhibit the same kind of "emanation" seen in the continuation simulations of Figures 3.2, 3.3, and 3.4, but a priori their geometries are more complex. We prove in Chapter 4 that the reduced Hamiltonian H_{xy} (2.27) has six relative equilibria corresponding to pairings of the Lagrange points L_1 - L_5 (cf. Fig. 1.1) generated by the primaries. Of these pairings, only those corresponding to the collinear points $L_1 - L_3$ are Lyapunov centers. This is an artifact of the equal-pair condition; there is numerical evidence that the L_4 and L_5 configurations are also Lyapunov centers when the primary masses have a certain critical ratio. The issue of L_4 and L_5 will be discussed in Chapter 6.

Despite the existence of Lyapunov orbits about the collinear centers, numerical simulation suggests that they are extremely unstable and only exist in tight orbits about their equilibria. This means we cannot give an illustrative to-scale graph of any of these orbits. At best, we can only refer to the diagram of Fig. 2.1 for exaggerated behavior.

Of particular interest are the "central-Hill" orbits about the system barycenter under the equal-pair condition. These are not quite Lyapunov orbits around the $L_1 - L_1$ equilibrium pairing (explored in the next chapter), but they are close in that the asteroids orbit just inside or just outside the equilibrium positions. Figure 3.5 displays an example of these central-Hill orbits.

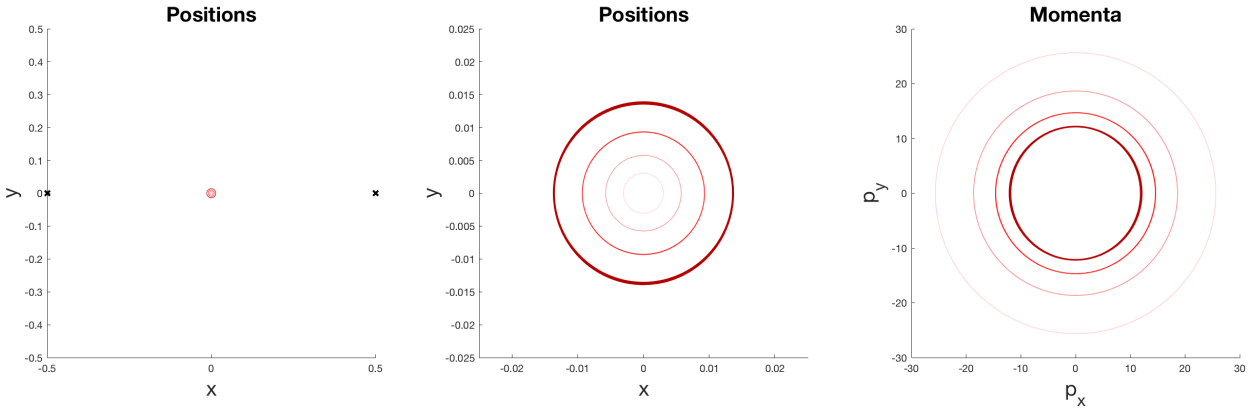

Figure 3.5 Continuation of near-circular central-Hill orbits under the equal-pair condition (2.20). Here both asteroids orbit about the system barycenter between the primaries. The left panel is the smallest field of view containing the primaries; the middle is zoomed in to better display the details. Notice the geometric similarities with Fig. 3.2.

Chapter 4

Relative Equilibria of the H_{xy} Problem

The first major analytical result of this thesis is the determination of the relative equilibria in the equations of motion

$$\begin{aligned}
\dot{x} &= \frac{p_x}{2m} + \frac{2\pi y}{P}, \\
\dot{y} &= \frac{p_y}{2m} - \frac{2\pi x}{P}, \\
\dot{p}_x &= \frac{2\pi p_y}{P} - \frac{mM(x-a/2)}{((x-\frac{a}{2})^2+y^2)^{3/2}} - \frac{mM(x+a/2)}{((x+\frac{a}{2})^2+y^2)^{3/2}} - \frac{m^2 x}{2(x^2+y^2)^{3/2}} \\
\dot{p}_y &= -\frac{2\pi p_x}{P} - \frac{mMy}{((x-\frac{a}{2})^2+y^2)^{3/2}} - \frac{mMy}{((x+\frac{a}{2})^2+y^2)^{3/2}} - \frac{m^2 y}{2(x^2+y^2)^{3/2}}
\end{aligned}$$

for the H_{xy} Hamiltonian

$$\begin{aligned}
H_{xy}(x,y,p_x,p_y) = \frac{1}{4m}\left(p_x^2+p_y^2\right) - \frac{2\pi}{P}\left(xp_y - yp_x\right) - \frac{m^2}{2\sqrt{x^2+y^2}} \\
- \frac{mM}{\sqrt{(x+a/2)^2+y^2}} - \frac{mM}{\sqrt{(x-a/2)^2+y^2}}
\end{aligned}$$

(cf. Eqns. (2.26) and (2.27)). The relative equilibria occur where the derivatives $\dot{x}, \dot{y}, \dot{p}_x, \dot{p}_y$ are all identically zero. Once combined with the COM variable solution $\alpha = \beta = p_\alpha = p_\beta = 0$ in the COM Binary Asteroid (2.23), this process will yield examples of relative equilibria in the full Binary Asteroid problem.

Because the H_{xy} Hamiltonian system is identical in form to the restricted 4-body problem in Llibre et al. [8], our results are qualitatively the same as theirs, but with changes according to different constants. As such, we shall present a derivation of our results consistent with our notation.

4.1 Amended Potential

Setting the $\dot{x}$ and $\dot{y}$ equations to be zero implies that

$$p_x = -\frac{4\pi my}{P} \text{ and } p_y = \frac{4\pi mx}{P}. \tag{4.1}$$

Substitute into the $\dot{p}_x$ and $\dot{p}_y$ equations, and set these to zero as well:

$$\begin{aligned} 0 = \dot{p}_x &= \frac{(4\pi^2)\cdot 2mx}{P^2} - \frac{mM(x-a/2)}{((x-\frac{a}{2})^2+y^2)^{3/2}} - \frac{mM(x+a/2)}{((x+\frac{a}{2})^2+y^2)^{3/2}} - \frac{m^2 x}{2(x^2+y^2)^{3/2}} \\ 0 = \dot{p}_y &= \frac{(4\pi^2)\cdot 2my}{P^2} - \frac{mMy}{((x-\frac{a}{2})^2+y^2)^{3/2}} - \frac{mMy}{((x+\frac{a}{2})^2+y^2)^{3/2}} - \frac{m^2 y}{2(x^2+y^2)^{3/2}}. \end{aligned} \tag{4.2}$$

On closer inspection, the right hand sides of (4.1) are actually the components of the x,y-gradient of the function $V(x,y)$ given by

$$V(x,y) = \frac{mM}{a^3}\left(x^2+y^2\right) + \frac{mM}{\sqrt{(x-\frac{a}{2})^2+y^2}} + \frac{mM}{\sqrt{(x+\frac{a}{2})^2+y^2}} + \frac{m^2}{2\sqrt{x^2+y^2}}. \tag{4.3}$$

The function $V(x,y)$ is called the "amended potential" for the H_{xy} system. It is of great use because according to Eqns. (4.1) and (4.2), we have that

$$\dot{x} = \dot{y} = \dot{p}_x = \dot{p}_y \equiv 0 \text{ if and only if } p_x = -\frac{4\pi my}{P} \text{ and } p_y = \frac{4\pi mx}{P} \text{ and } \nabla V(x,y) = (0,0),$$

or in other words, if the point $(x_0, y_0, p_{x_0}, p_{y_0})$ in phase space is a relative equilibrium, then (x_0, y_0) is a critical point of V. This is analogous to other physical systems: force is the (negative) gradient of potential energy, hence there is no force at any critical point of the potential, and any particle placed there will not move.

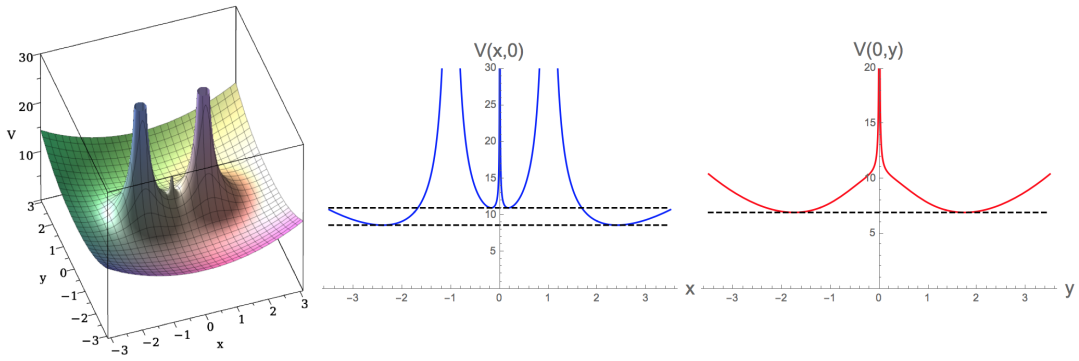

Figure 4.1 Graphs of several views of the amended potential $V(x,y)$, using the parameters $m = 0.5, M = 10$, and $a = 2$. (Left) Surface plot of $V(x,y)$. Relative equilibria of H_{xy} occur wherever the graphed surface is parallel to the xy-plane. (Middle) Cross-section plot of $V(x,0)$. The black dashed lines mark minima. (Right) Cross-section plot of $V(0,y)$.

This physics correspondence suggests that the amended potential V plays a larger role in the dynamics of H_{xy} than being a generator of equilibria. We can demonstrate this role by turning the equations of motion into second-order differential equations in the space coordinates x, y only. Differentiating the $\dot{x}$ equation yields

$$\begin{aligned}
\ddot{x} &= \frac{\dot{p}_x}{2m} + \frac{2\pi\dot{y}}{P} = \frac{1}{2m}\left[\frac{2\pi p_y}{P} + \frac{\partial V}{\partial x} - \frac{2mMx}{a^3}\right] + \frac{2\pi\dot{y}}{P} \\
&= \frac{\pi}{mP}\left[2m\dot{y} + \frac{4\pi mx}{P}\right] - \frac{Mx}{a^3} + \frac{2\pi\dot{y}}{P} + \frac{1}{2m}\frac{\partial V}{\partial x} \\
&= \frac{4\pi^2 x}{P^2} - \frac{Mx}{a^3} + \frac{4\pi\dot{y}}{P} + \frac{1}{2m}\frac{\partial V}{\partial x} \\
&= \frac{4\pi\dot{y}}{P} + \frac{1}{2m}\frac{\partial V}{\partial x}.
\end{aligned}$$

Differentiating $\dot{y}$ similarly gives

$$\begin{aligned}
\ddot{y} &= \frac{\dot{p}_y}{2m} - \frac{2\pi\dot{x}}{P} = \frac{1}{2m}\left[-\frac{2\pi p_x}{P} + \frac{\partial V}{\partial y} - \frac{2mMy}{a^3}\right] - \frac{2\pi\dot{x}}{P} \\
&= -\frac{\pi}{mP}\left[2m\dot{x} - \frac{4\pi my}{P}\right] - \frac{My}{a^3} - \frac{2\pi\dot{x}}{P} + \frac{1}{2m}\frac{\partial V}{\partial y} \\
&= \frac{4\pi^2 y}{P^2} - \frac{My}{a^3} - \frac{4\pi\dot{x}}{P} + \frac{1}{2m}\frac{\partial V}{\partial y} \\
&= -\frac{4\pi\dot{x}}{P} + \frac{1}{2m}\frac{\partial V}{\partial y}.
\end{aligned}$$

Therefore, the equations of motion are equivalent to the second-order equations

$$\begin{aligned} \ddot{x} - \frac{4\pi\dot{y}}{P} &= \frac{1}{2m}\frac{\partial V}{\partial x} \\ \ddot{y} + \frac{4\pi\dot{x}}{P} &= \frac{1}{2m}\frac{\partial V}{\partial y}. \end{aligned} \tag{4.4}$$

More simplification can be obtained from the modified equations of motion (4.4) by multiplying the $\ddot{x}$ equation by $\dot{x}$, multiplying the $\ddot{y}$ equation by $\dot{y}$, and adding:

$$\frac{d}{dt}\left[\frac{1}{2}\left(\dot{x}^2+\dot{y}^2\right)\right] = \dot{x}\ddot{x}+\dot{y}\ddot{y} = \frac{1}{2m}\left[\frac{\partial V}{\partial x}\dot{x}+\frac{\partial V}{\partial y}\dot{y}\right] = \frac{d}{dt}\left[\frac{V(x,y)}{2m}\right].$$

Integrating this relation with respect to time therefore reveals a conserved quantity for the system:

$$\frac{V(x,y)}{2m} - \frac{1}{2}\left(\dot{x}^2+\dot{y}^2\right) = C \tag{4.5}$$

where $C \in \mathbb{R}$ is a constant, typically called the "Jacobi constant." Notice that the level curves $V(x,y) = const.$ therefore dynamically correspond to curves where $\dot{x} = \dot{y} = 0$, called zero-velocity curves (ZVCs). Figure 4.2 displays some of these ZVCs for various values of the Jacobi constant C.

One can consider each ZVC as an envelope or extreme case of orbital behavior. By (4.5), an orbit can never penetrate the ZVC corresponding to the fixed value of the Jacobi constant, because if the ZVC were reached, then there would be no velocity and the system would remain in an equilibrium. This implies that we can determine "forbidden regions" that the asteroids cannot penetrate, given initial conditions.

4.2 Critical Points of $V(x,y)$

We now discuss a few simple relative equilibria, where $\nabla V(x,y) = (0,0)$. There are two classes we shall consider. The first class is the collinear class, corresponding to $y = 0$, and the second class is the vertical class, corresponding to $x = 0$. They are characterized thusly because according to Eqn.

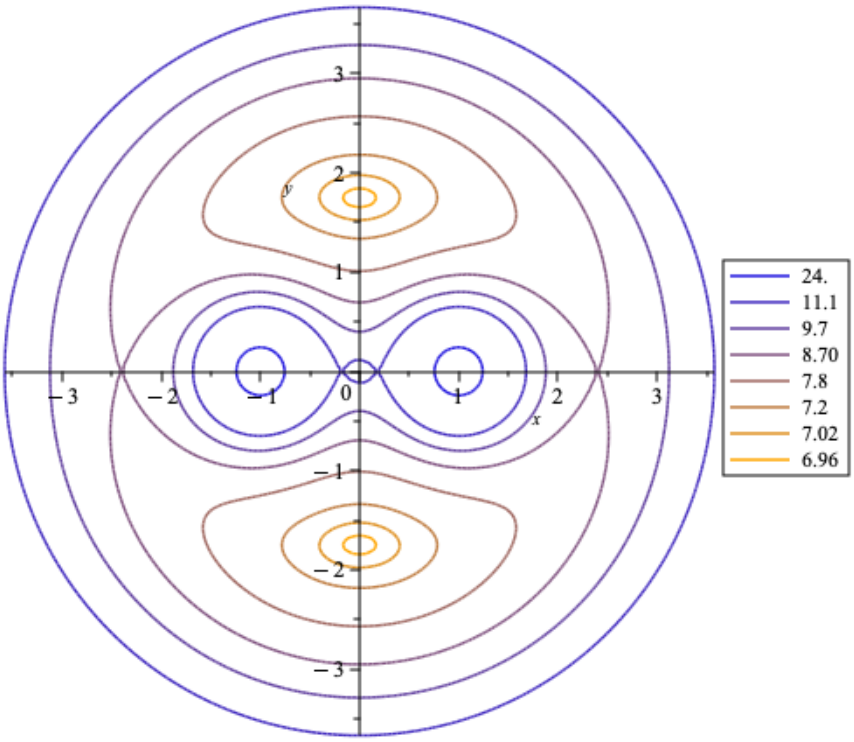

Figure 4.2 Zero-velocity curves for the H_{xy} system, according to Eqn. (4.5), using the parameters $m = 0.5, M = 10$, and $a = 2$. The legend displays the value of the Jacobi constant C.

(4.3),

$$\frac{\partial V}{\partial x}(0,y) = 0 - \frac{mM(0-a/2)}{((0-a/2)^2+y^2)^{3/2}} - \frac{mM(0+a/2)}{((0+a/2)^2+y^2)^{3/2}} - 0 = 0$$

and

$$\frac{\partial V}{\partial y}(x,0) = 0.$$

Therefore, our class conditions each automatically make one component of ∇V zero. It thus suffices to investigate the remaining components. Substituting, we find

$$\begin{aligned}\frac{\partial V}{\partial x}(x,0) &= \frac{2mMx}{a^3} - \frac{mM(x-a/2)}{|x-a/2|^3} - \frac{mM(x+a/2)}{|x+a/2|^3} - \frac{m^2 x}{2|x|^3}\\ \frac{\partial V}{\partial y}(0,y) &= \frac{2mMy}{a^3} - \frac{2mMy}{(y^2+a^2/4)^{3/2}} - \frac{m^2 y}{2|y|^3}.\end{aligned} \tag{4.6}$$

The roots of the functions in (4.6) mark the collinear and the vertical equilibria, respectively. Notice that both $\frac{\partial V}{\partial x}(x,0)$ and $\frac{\partial V}{\partial y}(0,y)$ are even in their respective variables. Hence, it is only necessary to consider the cases when $x>0$ and $y>0$.

Using some calculus, we now arrive at our first major result.

Theorem 3. ***(Relative Equilibria of H_{xy})*** *The amended potential $V(x,y)$ has exactly four critical points of the form $(x,0)$ and exactly two of the form $(0,y)$, which we label $(\pm L_1,0)$, $(\pm L_2,0)$, and $(0,\pm L_4)$, respectively, where*

$$L_1 \in \left(0,\frac{a}{2}\right),\ L_2 \in \left(\frac{a}{2},\infty\right),\ \text{and } L_4 \in \left(\frac{\sqrt{3}a}{2},\infty\right).$$

Proof. Define new functions $V_x(x,m,M,a)$ and $V_y(y,m,M,a)$ by

$$\begin{aligned}V_x(x,m,M,a) &= \frac{1}{m}\frac{\partial V}{\partial x}(x,0) = \frac{2Mx}{a^3} - \frac{M(x-a/2)}{|x-a/2|^3} - \frac{M(x+a/2)}{|x+a/2|^3} - \frac{mx}{2|x|^3}\\ V_y(y,m,M,a) &= \frac{1}{m}\frac{\partial V}{\partial y}(0,y) = \frac{2My}{a^3} - \frac{2My}{(y^2+a^2/4)^{3/2}} - \frac{my}{2|y|^3}.\end{aligned} \tag{4.7}$$

These functions are continuously differentiable in the positive hyper-octant $x,y,m,M,a>0$ (with the exception that V_x is undefined at $x=\pm a/2$). The relevant partial derivatives for the next step are

$$\begin{aligned}\frac{\partial V_x}{\partial x}(x,m,M,a) &= \frac{1}{m}\frac{\partial^2 V}{\partial x^2}(x,0) = \frac{2M}{a^3} + \frac{2M}{|x-a/2|^3} + \frac{2M}{|x+a/2|^3} + \frac{m}{|x|^3}\\ \frac{\partial V_y}{\partial y}(y,m,M,a) &= \frac{1}{m}\frac{\partial^2 V}{\partial y^2}(0,y) = \frac{2M}{a^3} + \frac{2M(2y^2-a^2/4)}{(y^2+a^2/4)^{5/2}} + \frac{m}{|y|^3}.\end{aligned} \tag{4.8}$$

From Eqn. (4.8), notice that $\frac{\partial V_x}{\partial x}(x,m,M,a)>0$ for all $x,m,M,a>0$. Therefore, for fixed m,M,a, the function $V_x(x,m,M,a)$ is increasing in x, by the Mean Value Theorem. Thus, the

equation $V_x(x,m,M,a) = 0$ has at most one solution for x in each of the intervals $(0,a/2)$ and $(a/2,\infty)$. However, because we have the limits

$$\lim_{x\to 0^+} V(x,0) = \lim_{x\to \frac{a}{2}^+} V(x,0) = \lim_{x\to \frac{a}{2}^-} V(x,0) = \lim_{x\to\infty} V(x,0) = \infty$$

via Eqn. (4.3), it follows by continuity that $V(x,0)$ attains local minima in both intervals $(0,a/2)$ and $(a/2,\infty)$. These minima correspond to points where $\frac{\partial V}{\partial x}(x,0) = 0$. Hence, we conclude that the equation $V_x(x,m,M,a) = 0$ has two solutions $L_1 \in (0,a/2)$ and $L_2 \in (a/2,\infty)$, and these solutions are unique within their respective intervals.

Likewise, notice

$$V_y\left(\frac{\sqrt{3}a}{2}, m, M, a\right) = -\frac{2m}{3a^2}$$

by substitution into (4.7), and $y > \sqrt{3}a/2$ implies $\frac{\partial V_y}{\partial y}(y,m,M,a) > 0$. That is, $V_y(y,m,M,a)$ is increasing in y on the interval $[\sqrt{3}a/2,\infty)$. So the equation $V_y(y,m,M,a) = 0$ can have at most one solution for y there. Because we see

$$\lim_{y\to\infty} V_y(y,m,M,a) = \lim_{y\to\infty} \frac{2My}{a^3} = \infty,$$

continuity of V_y immediately implies that the equation $V_y(y,m,M,a) = 0$ with $y \in [\sqrt{3}a/2,\infty)$ has a unique solution $L_4 \in [\sqrt{3}a/2,\infty)$. □

We remark that the equilibria of Theorem 3 are smooth (i.e., infinitely differentiable) as functions of the parameters m, M, and a. Additionally, we have the limits

$$\lim_{m\to 0^+} L_1 = 0 \text{ and } \lim_{m\to 0^+} L_4 = \frac{\sqrt{3}a}{2}.$$

The proof of the smoothness is much lengthier than what we presented above, and so it is left to the journal publication version of this work in Bakker & Freeman [12].

Theorem 3 declares that the six points $(\pm L_1, 0)$, $(\pm L_2, 0)$, $(0, \pm L_4)$ are the position coordinates of relative equilibria in the H_{xy} system. We labeled them like the Lagrange points of the CR3BP

precisely because of the smoothness limits discussed above. Indeed, when $m = 0$, the governing equations $V_x(x,0,M,a) = 0$ and $V_y(y,0,M,a) = 0$ are precisely of the same form found in the CR3BP for the Lagrange points (cf. Section 4.3 in Meyer & Offin [1]).

For a geometric picture, observe the points on the x-axis of Fig. 4.2 where the ZVCs cross on themselves. The outermost left and right crossings occur at $\pm L_2$, while the innermost occur at $\pm L_1$. The points on the y-axis where the ZVCs contract into smaller and smaller circles occur at $\pm L_4$. In the original Binary Asteroid coordinates and relative to the classical picture, these equilibria correspond to the asteroids being paired at the primaries' $L_1 - L_1$ (our found L_1), at $L_2 - L_3$ (our L_2), and at $L_4 - L_5$ (our L_4).

4.3 Spectra of Equilibria

Having found some relative equilibria for the Binary Asteroid problem, we now examine the spectral stability of those points. In the language of Section 2.3.2, this means we shall compute the exponents of the equilibria and check whether they satisfy the Lyapunov Center Theorem.

For simplicity, it will be useful to write down the equations of motion (2.26) in terms of the amended potential:

$$\begin{aligned}
\dot{x} &= \frac{p_x}{2m} + \frac{2\pi y}{P}, \\
\dot{y} &= \frac{p_y}{2m} - \frac{2\pi x}{P}, \\
\dot{p}_x &= \frac{2\pi p_y}{P} - \frac{2mMx}{a^3} + \frac{\partial V}{\partial x}, \\
\dot{p}_y &= -\frac{2\pi p_x}{P} - \frac{2mMy}{a^3} + \frac{\partial V}{\partial y}.
\end{aligned} \tag{4.9}$$

This means that the linearization matrix A whose eigenvalues are the exponents of the equilibria is

$$A = \begin{bmatrix} 0 & \frac{2\pi}{P} & \frac{1}{2m} & 0 \\ -\frac{2\pi}{P} & 0 & 0 & \frac{1}{2m} \\ -\frac{2mM}{a^3} + \frac{\partial^2 V}{\partial x^2} & \frac{\partial^2 V}{\partial x \partial y} & 0 & \frac{2\pi}{P} \\ \frac{\partial^2 V}{\partial x \partial y} & -\frac{2mM}{a^3} + \frac{\partial^2 V}{\partial y^2} & -\frac{2\pi}{P} & 0 \end{bmatrix}. \tag{4.10}$$

To avoid carrying the partial derivatives everywhere, we shall make the following substitutions:

$$\omega = \frac{2\pi}{P} = \sqrt{\frac{M}{a^3}},\ \alpha = \frac{1}{2m}\frac{\partial^2 V}{\partial x^2},\ \beta = \frac{1}{2m}\frac{\partial^2 V}{\partial x \partial y},\ \gamma = \frac{1}{2m}\frac{\partial^2 V}{\partial y^2} \tag{4.11}$$

(the α and β here are not to be confused with the COM coordinates). This turns Eqn. (4.10) into the following:

$$A = \begin{bmatrix} 0 & \omega & \frac{1}{2m} & 0 \\ -\omega & 0 & 0 & \frac{1}{2m} \\ 2m(\alpha - \omega^2) & 2m\beta & 0 & \omega \\ 2m\beta & 2m(\gamma - \omega^2) & -\omega & 0 \end{bmatrix}.$$

The characteristic polynomial of A is

$$\det(zI - A) = z^4 + (4\omega^2 - \alpha - \gamma)z^2 + \alpha\gamma - \beta^2. \tag{4.12}$$

The roots of this polynomial are the exponents of the examined equilibrium. Because it is a quadratic in z^2, we must examine the discriminant and c-constant

$$\Delta = (4\omega^2 - \alpha - \gamma)^2 - 4(\alpha\gamma - \beta^2) \text{ and } c = \alpha\gamma - \beta^2 \tag{4.13}$$

in order to characterize the exponents as real, imaginary, or complex. If $\Delta > 0$, we obtain pure real or pure imaginary exponents (depending on c), and if $\Delta < 0$, the exponents are all complex.

4.3.1 Collinear Points

Since the collinear points have $y = 0$, Eqn. (4.8) combines with the equation

$$\frac{\partial^2 V}{\partial x \partial y} = \frac{3mMy(x-a/2)}{((x-a/2)^2+y^2)^{5/2}} + \frac{3mMy(x+a/2)}{((x+a/2)^2+y^2)^{5/2}} + \frac{3m^2xy}{2(x^2+y^2)^{5/2}}$$

to get that

$$\alpha = \frac{M}{a^3} + \frac{m}{2|x|^3} + \frac{M}{|x-a/2|^3} + \frac{M}{|x+a/2|^3} > 0, \text{ and}$$
$$\beta = 0, \text{ and } \alpha + 2\gamma = \frac{3M}{a^3} = 3\omega^2$$

at $(L_1, 0)$ and $(L_2, 0)$. Equation (4.13) becomes

$$\Delta = \frac{1}{4}\left(9\alpha^2 - 34\alpha\omega^2 + 25\omega^4\right) = \frac{1}{4}\left(9\alpha - 25\omega^2\right)\left(\alpha - \omega^2\right),$$
$$c = -\frac{1}{2}\alpha(\alpha - 3\omega^2). \tag{4.14}$$

Because $9\alpha - 25\omega^2 = 9(\alpha - 3\omega^2) + 2\omega^2$, all we must do is examine the signs of $\alpha - \omega^2$, $9\alpha - 25\omega^2$, and $\alpha - 3\omega^2$. Substitution reveals that

$$\alpha - \omega^2 = \frac{m}{2|x|^3} + \frac{M}{|x-a/2|^3} + \frac{M}{|x+a/2|^3} > 0,$$
$$\alpha - 3\omega^2 = -\frac{3M}{a^3} + \frac{m}{2|x|^3} + \frac{M}{|x-a/2|^3} + \frac{M}{|x+a/2|^3}. \tag{4.15}$$

From here, some calculus is needed to finish and prove our next major result.

Theorem 4. ***(Collinear Spectra)*** *The collinear critical points $(\pm L_1, 0), (\pm L_2, 0)$ of the amended potential each have two real and two pure imaginary exponents as long as $m \leq 0.26427M$. Therefore, they are each Lyapunov centers according to Theorem 2.*

Proof. Consider the function $g(z)$ given by

$$g(z) = \frac{1}{|z-1/2|^3} + \frac{1}{|z+1/2|^3}. \tag{4.16}$$

Notice that $g(0) = 16$ and $g(1.209505) = 3.00001$. Additionally, g is continuously differentiable with positive derivative on $(0, 1/2)$ and negative derivative on $(1/2, \infty)$. Therefore, g is increasing on the former interval and decreasing on the latter. It follows that

$$g(z) \geq 16 \text{ for all } z \in [0, 1/2) \text{ and } g(z) \geq 3.00001 \text{ for all } z \in (0.5, 1.209505].$$

Applying this to Eqn. (4.15), we find that $\alpha - 3\omega^2 > 0$ at $(\pm L_1, 0)$ because $L_1/a \in [0, 1/2)$ by Theorem 3 and so $g(L_1/a) - 3 \geq 13 > 0$.

We can reach a similar conclusion if we can show that $L_2/a \in (0.5, 1.209505]$. We already know that $L_2/a > 0.5$ by Theorem 3. Recall from the proof of that theorem that the function V_x of Eqn. (4.7) is increasing for $x \in (a/2, \infty)$. Furthermore, substitution reveals

$$V_x(1.209505a, m, M, a) = \frac{-0.341786m + 0.090324M}{a^2}.$$

The hypothesis that $m \leq 0.26427M$ therefore implies that $V_x(1.209505a, m, M, a) > 0$.

Since V_x is increasing, this latter fact implies that the solution $V_x(L_2, m, M, a) = 0$ must occur before $x = 1.209505a$. Therefore, $L_2/a < 1.209505$ as desired. The same logic as L_1 allows us to conclude that $\alpha - 3\omega^2 > 0$ at $(\pm L_2, 0)$, because $g(L_2/a) - 3 \geq 0.00001$.

Finally, since $\alpha, \alpha - 3\omega^2 > 0$ at the collinear critical points, Eqn. (4.14) says that $\Delta > 0$ and $c < 0$. By the quadratic formula, the polynomial $w^2 + (4\omega^2 - \alpha - \gamma)w + c$ has one positive and one negative real root. Therefore, the characteristic polynomial (4.12) has one positive real root, one negative real root, and two conjugate pure imaginary roots. □

4.3.2 Vertical Points

The vertical points have $x = 0$. Similar to the previous subsection, we have $\beta = 0$ and

$$\begin{aligned} \alpha &= \frac{M}{a^3} - \frac{m}{4|y|^3} + M\left[\frac{3a^2/4}{(y^2 + a^2/4)^{5/2}} - \frac{1}{(y^2 + a^2/4)^{3/2}}\right], \\ \gamma &= \frac{M}{a^3} + \frac{m}{2|y|^3} + M\left[\frac{3y^2}{(y^2 + a^2/4)^{5/2}} - \frac{1}{(y^2 + a^2/4)^{3/2}}\right]. \end{aligned} \tag{4.17}$$

By dividing Eqn. (4.6) by $2my$, the y coordinates of the vertical points satisfy

$$0 = \frac{M}{a^3} - \frac{M}{(y^2+a^2/4)^{3/2}} - \frac{m}{4|y|^3}. \tag{4.18}$$

Together, these equations give the analogue of Theorem 4 for the vertical points.

Theorem 5. ***(Vertical Spectra)*** *The vertical critical points $(0, \pm L_4)$ of the amended potential each have four complex exponents. as long as $m \leq 1.13783M$. Therefore, they are not Lyapunov centers.*

Proof. The proof is similar to that of Theorem 4. Consider the function $h(z)$ given by

$$h(z) = 1 - \frac{9z^2}{(z^2+1/4)^5} \tag{4.19}$$

h is continuously differentiable everywhere with positive derivative on the interval $(\sqrt{3}/2, 1)$. Therefore, h is increasing on $[\sqrt{3}/2, 1]$. Since $h(1) = -1.94912 < 0$, this implies $h(z) < 0$ for all $z \in [\sqrt{3}/2, 1]$.

Subtract (4.18) from (4.17) to get

$$\begin{aligned} \alpha &= \frac{3Ma^2}{4(y^2+a^2/4)^{5/2}} > 0, \\ \gamma &= \frac{3m}{4|y|^3} + \frac{3My^2}{(y^2+a^2/4)^{5/2}} > 0. \end{aligned} \tag{4.20}$$

This implies the c constant is $c = \alpha\gamma > 0$. We also obtain

$$\alpha + \gamma = \frac{3m}{4|y|^3} + \frac{3M}{(y^2+a^2/4)^{3/2}} = \frac{3M}{a^3} = 3\omega^2.$$

It follows that the discriminant Δ satisfies

$$\Delta = \frac{M^2}{a^6} - \frac{3Ma^2}{(y^2+a^2/4)^{5/2}}\left[\frac{3m}{4|y|^3} + \frac{3My^2}{(y^2+a^2/4)^{5/2}}\right] < \frac{M^2}{a^6}\left[1 - \frac{9(y/a)^2}{((y/a)^2+1/4)^5}\right] = \frac{M^2}{a^6} h\left(\frac{y}{a}\right).$$

Once we demonstrate that $L_4/a \in [\sqrt{3}/2, 1]$, the above work regarding h will imply that $\Delta < 0$.

We already know that $L_4/a > \sqrt{3}/2$ by Theorem 3. Recall from the proof of that theorem that the function V_y of (4.7) is increasing in y on the interval $[\sqrt{3}a/2, \infty)$. However, substitution reveals that

$$V_y(a, m, M, a) = \frac{-0.5m + 0.568916M}{a^2}.$$

The hypothesis that $m \leq 1.13783M$ therefore implies that $V_y(a,m,M,a) > 0$. Hence, the solution $V_y(L_4,m,M,a) = 0$ must occur before $y = a$; we have $L_4/a < 1$ as desired.

Now we conclude $\Delta < M^2 h(L_4/a)/a^6 < 0$ at $(0,\pm L_4)$. By the quadratic formula, the polynomial $w^2 + (4\omega^2 - \alpha - \gamma)w^2 + c$ has two complex roots. Therefore, the characteristic polynomial (4.12) has four complex roots. □

To summarize, we have successfully computed (cf. Theorem 3) six relative equilibria of the H_{xy} system, at positions $(\pm L_1,0),(\pm L_2,0)$, and $(0,\pm L_4)$. For physical situations (i.e., $m \ll M$), we found that the collinear points L_1 and L_2 are Lyapunov centers (cf. Theorem 4) and the vertical point L_4 has four complex exponents (Theorem 5). We remark that although the Lyapunov Center Theorem applies to L_1 and L_2, the fact that they have real exponents means their Lyapunov orbits are very unstable.

Chapter 5

Hill and Comet Orbits

The second major analytical result of this thesis is the investigation of the Hill and comet orbits discussed in brief in Chapter 3. We prove the existence of one-parameter families of near-circular periodic orbits of both types, making use of Theorem 1. Additionally, we examine "central-Hill" orbits about the system barycenter enveloping or contained within the L_1 equilibrium from Theorem 3.

5.1 Hill Scaling

As displayed in Fig. 3.2, the Hill orbits in the original coordinates have each asteroid orbit one primary separately. They are named after astronomer George William Hill who studied such orbits in the context of the Earth-Moon-Sun system [13]. To find periodic Hill orbits arising from the equal-pair condition (2.20), we utilize the H_{xy} Hamiltonian system (2.27) and implement a symplectic scaling to zoom into a singularity of the amended potential.

5.1.1 Zooming Into Primary

We shall zoom into the left primary at $(x,y) = (-a/2, 0)$. Similar work could be used at the right primary; due to symmetry it is sufficient to consider one case. Because the scaling of Eqn. (2.12) requires us to center our zoom at the origin, we first translate our coordinate frame so that the left primary is at the origin. The translation is:

$$x' = x + \frac{a}{2}, \qquad y' = y, \qquad p'_x = p_x, \qquad p'_y = p_y + \frac{2\pi am}{P}. \tag{5.1}$$

As in Section 2.2.1, the primes denote new variables, not derivatives. The point $(x', y') = (0,0)$ now corresponds to $(x,y) = (0,0)$. We note that we shifted the p_y momentum to eliminate unfavorable terms in the Hamiltonian substitution.

This translation is symplectic as a coordinate transformation, because the Jacobian is just the identity matrix. Hence, the H_{xy} Hamiltonian (2.27) substitutes into

$$\begin{aligned} H_{xy} = \frac{1}{4m}\left((p'_x)^2 + (p'_y)^2\right) - \frac{2\pi}{P}\left(x'p'_y - y'p'_x\right) + \frac{4\pi^2 amx'}{P^2} - \frac{\pi^2 a^2 m}{P^2} \\ - \frac{m^2}{2\sqrt{(x'-a/2)^2 + (y')^2}} - \frac{mM}{\sqrt{(x')^2 + (y')^2}} - \frac{mM}{\sqrt{(x'-a)^2 + (y')^2}}. \end{aligned} \tag{5.2}$$

Notice that because the equations of motion (1.1) depend on the derivatives of th Hamiltonian, the constant $-\pi^2 a^2 m/P^2$ in (5.2) can be ignored.

Now we implement a symplectic scaling in the form of Eqn. (2.12). Let $\delta > 0$ be a (small) parameter, and define the inverse scaling transformation

$$x' = \delta^2 \xi, \qquad y' = \delta^2 \eta, \qquad p'_x = \delta^{-1} p_\xi, \qquad p'_y = \delta^{-1} p_\eta. \tag{5.3}$$

In the limit as $\delta \to 0$, we see that x' and y' approach zero, that is, we force the left asteroid to orbit the left primary. The forward transformation $(x', y', p'_x, p'_y) \mapsto (\xi, \eta, p_\xi, p_\eta)$ has multiplier δ^{-1}.

Hence, Eqn. (2.11) says that the new Hamiltonian $H_{\xi\eta}$ is (upon ignoring the constant $-\pi^2 a^2 m/P^2$):

$$H_{\xi\eta} = \delta^{-1} H_{xy} = \frac{\delta^{-3}}{4m}\left(p_\xi^2 + p_\eta^2\right) - \frac{2\pi}{P}\left(\xi p_\eta - \eta p_\xi\right) + \frac{\delta m M \xi}{a^2} - \frac{\delta^{-3} m M}{\sqrt{\xi^2+\eta^2}} - \frac{\delta^{-1} m^2}{2\sqrt{(\delta^2\xi - a/2)^2 + (\delta^2\eta)^2}} - \frac{\delta^{-1} m M}{\sqrt{(\delta^2\xi - a)^2 + (\delta^2\eta)^2}}. \tag{5.4}$$

In the equations of motion (1.1), we can make a "time scaling" $\tau = \delta^{-3} t$ to change all derivatives with respect to the original time t into derivatives with respect to τ. By the Chain Rule,

$$\frac{d}{d\tau} = \frac{dt}{d\tau}\cdot\frac{d}{dt} = \delta^3 \frac{d}{dt}.$$

That is, the effect on the equations of motion is to multiply every equation by δ^3. Making this time scaling therefore produces a new Hamiltonian system with Hamiltonian $\delta^3 H_{\xi\eta}$. Physically, our time scaling slows down the dynamics of the orbit; we'll see that the orbits speed up as they get closer and closer to the singularity at the primary.

Grouping the terms of $\delta^3 H_{\xi\eta}$ according to their powers of δ gives

$$\delta^3 H_{\xi\eta} = \left[\frac{1}{4m}\left(p_\xi^2 + p_\eta^2\right) - \frac{mM}{\sqrt{\xi^2+\eta^2}}\right] - \delta^3\left[\frac{2\pi}{P}\left(\xi p_\eta - \eta p_\xi\right)\right] + \delta^4\left[\frac{mM\xi}{a^2}\right] - \delta^2\left[\frac{m^2}{2\sqrt{(\delta^2\xi - a/2)^2 + (\delta^2\eta)^2}} + \frac{mM}{\sqrt{(\delta^2\xi - a)^2 + (\delta^2\eta)^2}}\right].$$

This expression is analytic in δ about $\delta = 0$. Expanding in a Taylor series about zero reveals the perturbative nature of our scaling:

$$\delta^3 H_{\xi\eta} = H_0 - \frac{\delta^2 m(m+M)}{a} + \delta^3 H_3 + \delta^4 H_4 + O(\delta^6), \tag{5.5}$$

where

$$H_0 = \frac{1}{4m}\left(p_\xi^2 + p_\eta^2\right) - \frac{mM}{\sqrt{\xi^2+\eta^2}}, \qquad H_3 = -\frac{2\pi}{P}\left(\xi p_\eta - \eta p_\xi\right), \qquad H_4 = -\frac{2m^2\xi}{a^2}. \tag{5.6}$$

As before, we ignore the constant $-\delta^2 m(m+M)/a$ since it does not affect the equations of motion.

The Taylor series expansion (5.5) reveals that the Hamiltonian system $\delta^3 H_{\xi\eta}$ is an order-δ^3 perturbation of the system H_0, or equivalently an order-δ^4 perturbation of $H_0 + \delta^3 H_3$. Our goal is to demonstrate that certain periodic solutions of $H_0 + \delta^3 H_3$ are in fact elementary, and thus continue into the $H_{\xi\eta}$ system via Theorem 1.

5.1.2 Polar Coordinates and Circular Orbits

The periodic solutions of interest in the $H_0 + \delta^3 H_3$ system are circular, because as one may check, that system is a version of the rotating 2-body problem. To verify this rigorously, we shall write Eqn. (5.5) in symplectic polar coordinates (see Section 2.1.2).

The polar coordinates we use are simply given by Eqns. (2.8) and (2.9):

$$\xi = r\cos\theta, \qquad \eta = r\sin\theta, \qquad p_\xi = p_r\cos\theta - \frac{p_\theta}{r}\sin\theta, \qquad p_\eta = p_r\sin\theta + \frac{p_\theta}{r}\cos\theta.$$

The Hamiltonian $\delta^3 H_{\xi\eta}$ becomes

$$\delta^3 H_{\xi\eta} = \frac{1}{4m}\left(p_r^2 + \frac{p_\theta^2}{r^2}\right) - \frac{mM}{r} - \delta^3\frac{2\pi p_\theta}{P} + O(\delta^4), \tag{5.7}$$

and thus, the equations of motion (1.1) in the new time τ are

$$\begin{aligned}
\frac{dr}{d\tau} &= \frac{\partial(\delta^3 H_{\xi\eta})}{\partial p_r} &&= \frac{p_r}{2m} + O(\delta^4),\\
\frac{d\theta}{d\tau} &= \frac{\partial(\delta^3 H_{\xi\eta})}{\partial p_\theta} &&= \frac{p_\theta}{2mr^2} - \frac{2\pi\delta^3}{P} + O(\delta^4),\\
\frac{dp_r}{d\tau} &= -\frac{\partial(\delta^3 H_{\xi\eta})}{\partial r} &&= \frac{p_\theta^2}{2mr^3} - \frac{mM}{r^2} + O(\delta^4),\\
\frac{dp_\theta}{d\tau} &= -\frac{\partial(\delta^3 H_{\xi\eta})}{\partial \theta} &&= O(\delta^4).
\end{aligned} \tag{5.8}$$

By ignoring the order-δ^4 terms and higher, we find that the p_θ solution is $p_\theta(\tau) = const$. This is precisely the conservation of angular momentum mentioned in Section 2.1.2. We therefore have liberty in choosing the value of the p_θ constant, say $p_\theta(\tau) = c$.

To find a circular solution to Eqn. (5.8), we want to force $r(\tau) = const$. Doing so forces $dr/d\tau = 0$ and thus $p_r(\tau) = 0$. Now the p_r equation becomes $dp_r/d\tau = 0$, giving an equation for the constant r:

$$0 = \frac{c^2}{2mr^3} - \frac{mM}{r^2} \implies r(\tau) = \frac{(c/m)^2}{2M}.$$

Therefore, a circular periodic solution to Eqn. (5.8) out to order-δ^3 is

$$r(\tau) = \frac{(c/m)^2}{2M}, \qquad \theta(\tau) = \theta_0 + \left(\frac{2M^2}{(c/m)^3} - \frac{2\pi}{P}\delta^3 \right) \tau, \qquad p_r(\tau) = 0, \qquad p_\theta(\tau) = c. \tag{5.9}$$

The τ-period $T > 0$ is 2π over the angular frequency in the θ solution:

$$T = \left| \frac{2\pi}{\frac{2M^2}{(c/m)^3} - \frac{2\pi}{P}\delta^3} \right| = \left| \frac{2\pi(c/m)^3 P}{2M^2 P - 2\pi\delta^3 (c/m)^3} \right| = \left| \frac{\pi(c/m)^3}{M^2 P - \pi\delta^3 (c/m)^3} \right| P. \tag{5.10}$$

Notice that the value of T depends on the sign of c. This leads to the difference in positive and negative angular momentum Hill orbits mentioned in Section 3.2. For small enough δ, taking $c > 0$ implies the denominator of T is smaller, making T larger and the overall orbit slower. Likewise, taking $c < 0$ makes the denominator larger, making T smaller and the orbit quicker.

5.1.3 Continuation into Binary Asteroid

Recall that the circular solution (5.9) exists only if we ignore the order-δ^4 terms in the $\delta^3 H_{\xi\eta}$ system. That is, it is not the solution to the Binary Asteroid problem. However, we show that it is indeed a perturbation of a periodic solution. To do so, we require Theorem 1, and therefore, we must compute the multipliers of the periodic solution.

It can be shown (cf. Section 2.6.1 of [1]) that the monodromy matrix $\mathfrak{M}$ of the periodic solution (5.9) satisfies

$$\mathfrak{M} = \exp\left(T \cdot J_2 D^2 (H_0 + \delta^3 H_3) \right), \tag{5.11}$$

where D^2 is the Hessian matrix of second-order partials evaluated at the periodic solution, and we are utilizing the matrix exponential. We used the `D` function in Mathematica to compute the relevant

Hessian:

$$T \cdot J_2 D^2(H_0 + \delta^3 H_3) = T \begin{bmatrix} 0 & 0 & \frac{1}{2m} & 0 \\ -\frac{p_\theta}{mr^3} & 0 & 0 & \frac{1}{2mr^2} \\ \frac{2mM}{r^3} - \frac{3p_\theta^2}{2mr^4} & 0 & 0 & \frac{p_\theta}{mr^3} \\ 0 & 0 & 0 & 0 \end{bmatrix} = \begin{bmatrix} 0 & 0 & \frac{T}{2m} & 0 \\ -\frac{8M^3T}{(c/m)^5} & 0 & 0 & \frac{2M^2T}{m(c/m)^4} \\ -\frac{8mM^4T}{(c/m)^6} & 0 & 0 & \frac{8M^3T}{(c/m)^5} \\ 0 & 0 & 0 & 0 \end{bmatrix}. \tag{5.12}$$

By a well-known fact about matrix exponentials, the multipliers, being the eigenvalues of $\mathfrak{M}$ are just e raised to the eigenvalues of $T \cdot J_2 D^(H_0 + \delta^3 H_3)$. The characteristic polynomial of this latter matrix (5.12) was found by Mathematica to be

$$Q(z) = z^2 \left(z^2 + \frac{4M^4T^2}{(c/m)^6} \right),$$

which has roots

$$z_1 = z_2 = 0 \text{ and } z_3 = -z_4 = \frac{2M^2Ti}{(c/m)^3}$$

(since $4M^4T^2/(c/m)^6 > 0$).

So, by Eqn. (5.11), the multipliers of (5.9) are

$$\lambda_{1,2} = +1, \qquad \lambda_{3,4} = \exp\left(\pm \frac{2M^2Ti}{(c/m)^3} \right) = 1 \pm 2\pi i \left(\frac{\pi (c/m)^3}{M^2 P} \right) \delta^3 + O(\delta^6) \tag{5.13}$$

as long as $M^2T/(c/m)^3$ is not an integer multiple of π. Since there are only countably many integers, this creates only a countable number of disallowed choices for c.

We conclude that the periodic solution (5.9) to $H_0 + \delta^3 H_3$ is elementary whenever $\delta > 0$, because then $+1$ is a multiplier exactly twice. Now Theorem 1 gives us our next major result.

Theorem 6. ***(Periodic Hill Orbits)*** *For almost every $c > 0$, there exist two one-parameter families of near-circular periodic solutions to the Binary Asteroid Problem* (2.18) *under the equal-pair condition* (2.20)*, where each asteroid orbits near one primary. The parameter is the symplectic scale factor $\delta > 0$ and the families are characterized by having positive or negative angular momentum $p_\theta = \pm c$.*

Proof. By Theorem 1, Equation (5.13), and the continuation argument in Section 9.4 of Meyer & Offin [1], the solution Eqn. (5.9) continues in the parameter δ to a periodic solution of the $\delta^3 H_{\xi\eta}$ Hamiltonian (5.4).

Convert this continued solution into the original x,y coordinates to get a periodic solution $(x,y,p_x,p_y) = (x^*(t),y^*(t),p_x^*(t),p_y^*(t))$ of the H_{xy} system (2.27). Following the work of Section 2.2.2, this implies that

$$(x_1,y_1,x_2,y_2,p_{x_1},p_{y_1},p_{x_2},p_{y_2}) = \left(x^*(t),y^*(t),-x^*(t),-y^*(t),\frac{p_x^*(t)}{2},\frac{p_y^*(t)}{2},-\frac{p_x^*(t)}{2},-\frac{p_y^*(t)}{2}\right)$$

is a periodic solution to the full Binary Asteroid Problem (2.18). □

We remark that the continuation process for the Hill orbits can be seen in Fig. 3.2. The darkening of hue corresponds to increasing the parameter δ.

5.2 Hill-Type Orbits About L_1

In the previous section, we did not have to zoom into the left primary. We could have zoomed into the singularity at the x,y-origin, which physically corresponds to the barycenter of the primaries and asteroids, or alternatively, the L_1 equilibrium of Theorem 3. Doing so yields similar work, but different results. Adapting the previous section, we implement a symplectic scaling, change to polar coordinates, and then solve the resultant equations of motion for a circular periodic solution. Once we have the solution, we compute the multipliers and use Theorem 1 to continue into the Binary Asteroid problem.

We begin with the original H_{xy} Hamiltonian (2.27), and implement a similar scaling as Eqn. (5.3):

$$x = \delta^2\xi, \qquad y = \delta^2\eta, \qquad p_x = \delta^{-1}p_\xi, \qquad p_y = \delta^{-1}p_\eta. \tag{5.14}$$

The Hamiltonian H_{xy} substitutes in a manner similar to (5.4):

$$H_{\xi\eta} = \delta^{-1}H_{xy} = \frac{\delta^{-3}}{4m}\left(p_\xi^2 + p_\eta^2\right) - \frac{2\pi}{P}\left(\xi p_\eta - \eta p_\xi\right) - \frac{\delta^{-3}m^2}{2\sqrt{\xi^2+\eta^2}} - \frac{\delta^{-1}mM}{\sqrt{(\delta^2\xi - a/2)^2 + (\delta^2\eta)^2}} - \frac{\delta^{-1}mM}{\sqrt{(\delta^2\xi + a/2)^2 + (\delta^2\eta)^2}}. \tag{5.15}$$

Scale time by $\tau = \delta^{-3}t$ to multiply the Hamiltonian by δ^3. Then expand the result in a Taylor series in δ, as in Eqns. (5.5) and (5.6):

$$\delta^3 H_{\xi\eta} = H_0 - \frac{4\delta^2 mM}{a} + \delta^3 H_3 + O(\delta^6), \tag{5.16}$$

where

$$H_0 = \frac{1}{4m}\left(p_\xi^2 + p_\eta^2\right) - \frac{m^2}{2\sqrt{\xi^2+\eta^2}}, \qquad H_3 = -\frac{2\pi}{P}\left(\xi p_\eta - \eta p_\xi\right). \tag{5.17}$$

As before, we may ignore the constant $-4\delta^2 mM/a$ since it does not contribute to the equations of motion.

Implement the same symplectic polar coordinates as before. Doing so makes the Hamiltonian (5.16)

$$\delta^3 H_{\xi\eta} = \frac{1}{4m}\left(p_r^2 + \frac{p_\theta^2}{r^2}\right) - \frac{m^2}{2r} - \delta^3\frac{2\pi p_\theta}{P} + O(\delta^6). \tag{5.18}$$

The equations of motion in the scaled time are

$$\begin{aligned}
\frac{dr}{d\tau} &= \frac{\partial(\delta^3 H_{\xi\eta})}{\partial p_r} &&= \frac{p_r}{2m} + O(\delta^6),\\
\frac{d\theta}{d\tau} &= \frac{\partial(\delta^3 H_{\xi\eta})}{\partial p_\theta} &&= \frac{p_\theta}{2mr^2} - \frac{2\pi\delta^3}{P} + O(\delta^6),\\
\frac{dp_r}{d\tau} &= -\frac{\partial(\delta^3 H_{\xi\eta})}{\partial r} &&= \frac{p_\theta^2}{2mr^3} - \frac{m^2}{2r^2} + O(\delta^6),\\
\frac{dp_\theta}{d\tau} &= -\frac{\partial(\delta^3 H_{\xi\eta})}{\partial \theta} &&= O(\delta^6).
\end{aligned} \tag{5.19}$$

These equations are (to order-δ^3) identical to Eqn. (5.8), except with M replaced with $m/2$ in the p_r equation. Therefore, a periodic circular solution to (5.19) is

$$r(\tau) = \frac{(c/m)^2}{m}, \qquad \theta(\tau) = \theta_0 + \left(\frac{2M^2}{(c/m)^3} - \frac{2\pi}{P}\delta^3\right)\tau, \qquad p_r(\tau) = 0, \qquad p_\theta(\tau) = c \tag{5.20}$$

with τ-period

$$T = \left| \frac{\pi (c/m)^3}{m^2 P/4 - \pi \delta^3 (c/m)^3} \right| P. \tag{5.21}$$

Additionally, using the same work as Section 5.1.3, we find that the multipliers of the solution are

$$\lambda_{1,2} = +1, \qquad \lambda_{3,4} = \exp\left(\pm \frac{m^2 T i}{2(c/m)^3} \right) = 1 \pm 2\pi i \left(\frac{4\pi (c/m)^3}{m^2 P} \right) \delta^3 + O(\delta^6). \tag{5.22}$$

Repeating the argument of Theorem 6 now gives us the existence of the central-Hill orbits.

Theorem 7. ***(Periodic Central-Hill Orbits)*** *For almost every $c > 0$, there exist two one-parameter families of near-circular periodic solutions to the Binary Asteroid Problem* (2.18) *under the equal-pair condition* (2.20)*, where the asteroids orbit together around the system barycenter. The parameter is the symplectic scale factor $\delta > 0$ and the families are characterized by having positive or negative angular momentum $p_\theta = \pm c$.*

Proof. See Theorem 6. □

The results of the central-Hill continuation can be seen in Fig. 3.5.

5.3 Comet Scaling

The final result of this chapter is the demonstration of the existence of periodic comet orbits seen in Fig. 3.2. We utilize the same general technique as the previous two sections, except we zoom out instead of in. We also abandon our use of the equal-pair condition (2.20), finding solutions for arbitrary choices of masses m_1, m_2, M_1, M_2 in the full Binary Asteroid problem (2.18).

The approach is the same as the previous two sections: scale, change to polar coordinates, find a circular solution, and then compute the multipliers. However, since we are doing this in the most general mass setting, there are some nuances that need to be addressed.

5.3.1 Zooming Out and Polar Coordinates

Following the work of the previous sections, let $\delta > 0$ be a small scaling parameter, and in the H_{BA} system (2.18), define the inverse transformation $(x_i, y_i, p_{x_i}, p_{y_i}) \mapsto (\xi_i, \eta_i, p_{\xi_i}, p_{\eta_i})$, $i = 1,2$, by

$$x_i = \delta^{-2}\xi_i, \qquad y_i = \delta^{-2}\eta_i, \qquad p_{x_i} = \delta p_{\xi_i}, \qquad p_{y_i} = \delta p_{\eta_i}. \tag{5.23}$$

This is symplectic with multiplier δ and the Hamiltonian H_{BA} becomes

$$\begin{aligned}\hat{H}_{BA} = \delta H_{BA} = &\frac{\delta^3}{2m_1}\left(p_{\xi_1}^2 + p_{\eta_1}^2\right) + \frac{\delta^3}{2m_2}\left(p_{\xi_2}^2 + p_{\eta_2}^2\right) - \frac{2\pi}{P}\left(\xi_1 p_{\eta_1} - \eta_1 p_{\xi_1}\right) \\ &- \frac{2\pi}{P}\left(\xi_2 p_{\eta_2} - \eta_2 p_{\xi_2}\right) - \frac{\delta^3 m_1 m_2}{\sqrt{(\xi_1-\xi_2)^2 + (\eta_1-\eta_2)^2}} \\ &- \frac{\delta^3 m_1 M_1}{\sqrt{(\xi_1 + a\delta^2 M_2/M)^2 + \eta_1^2}} - \frac{\delta^3 m_2 M_1}{\sqrt{(\xi_2 + a\delta^2 M_2/M)^2 + \eta_2^2}} \\ &- \frac{\delta^3 m_1 M_2}{\sqrt{(\xi_1 - a\delta^2 M_1/M)^2 + \eta_1^2}} - \frac{\delta^3 m_2 M_2}{\sqrt{(\xi_2 - a\delta^2 M_1/M)^2 + \eta_2^2}}.\end{aligned} \tag{5.24}$$

As in the Hill case, Eqn. (5.24) is analytic in δ at zero, so we may expand in a Taylor series:

$$\hat{H}_{BA} = H_0 + \delta^3 H_3 + O(\delta^7), \tag{5.25}$$

where

$$\begin{aligned}H_0 &= -\frac{2\pi}{P}\left(\xi_1 p_{\eta_1} - \eta_1 p_{\xi_1} + \xi_2 p_{\eta_2} - \eta_2 p_{\xi_2}\right), \\ H_3 &= \frac{1}{2m_1}\left(p_{\xi_1}^2 + p_{\eta_1}^2\right) + \frac{1}{2m_2}\left(p_{\xi_2}^2 + p_{\eta_2}^2\right) - \frac{m_1 M}{\sqrt{\xi_1^2 + \eta_1^2}} - \frac{m_2 M}{\sqrt{\xi_2^2 + \eta_2^2}} - \frac{m_1 m_2}{\sqrt{(\xi_1-\xi_2)^2 + (\eta_1-\eta_2)^2}}.\end{aligned} \tag{5.26}$$

We shall consider circular periodic solutions to the $H_0 + \delta^3 H_3$ system. To this end, it is use to convert to a "double polar" coordinate system. We use the same formulas as Eqns. (2.8) and (2.9). For $i = 1,2$:

$$\xi_i = r_i\cos(\theta_i), \quad \eta_i = r_i\sin(\theta_i), \quad p_{\xi_i} = p_{r_i}\cos(\theta_i) - \frac{p_{\theta_i}}{r_i}\sin(\theta_i), \quad p_{\eta_i} = p_{r_i}\sin(\theta_i) + \frac{p_{\theta_i}}{r_i}\cos(\theta_i).$$

This transformation is symplectic because the Jacobian is block-diagonal, with blocks equal to the Jacobians of the "single polar" transformation rule. Since those blocks are symplectic, the whole transformation is also.

In the polar coordinates, the Hamiltonian (5.24) becomes

$$\hat{H}_{BA} = H_0 + \delta^3 H_3 + O(\delta^7) = -\frac{2\pi}{P}(p_{\theta_1} + p_{\theta_2}) + \frac{\delta^3}{2m_1}\left(p_{r_1}^2 + \frac{p_{\theta_1}^2}{r_1^2}\right) + \frac{\delta^3}{2m_2}\left(p_{r_2}^2 + \frac{p_{\theta_2}^2}{r_2^2}\right) - \frac{\delta^3 m_1 M}{r_1} - \frac{\delta^3 m_2 M}{r_2} - \frac{\delta^3 m_1 m_2}{\sqrt{r_1^2 + r_2^2 - 2r_1 r_2 \cos(\theta_1 - \theta_2)}} + O(\delta^7). \tag{5.27}$$

The equations of motion (1.1) are

$$\begin{aligned}
\dot{r}_1 &= \frac{\delta^3 p_{r_1}}{m_1},\ \dot{r}_2 = \frac{\delta^3 p_{r_2}}{m_2},\\
\dot{\theta}_1 &= -\frac{2\pi}{P} + \frac{\delta^3 p_{\theta_1}}{m_1 r_1^2},\ \dot{\theta}_2 = -\frac{2\pi}{P} + \frac{\delta^3 p_{\theta_2}}{m_2 r_2^2},\\
\dot{p}_{r_1} &= \delta^3 \left[\frac{p_{\theta_1}^2}{m_1 r_1^3} - \frac{m_1 M}{r_1^2} - \frac{m_1 m_2 (r_1 - r_2\cos(\theta_1 - \theta_2))}{\sqrt{r_1^2 + r_2^2 - 2r_1 r_2 \cos(\theta_1 - \theta_2)}^3}\right],\\
\dot{p}_{r_2} &= \delta^3 \left[\frac{p_{\theta_2}^2}{m_2 r_2^3} - \frac{m_2 M}{r_2^2} - \frac{m_1 m_2 (r_2 - r_1\cos(\theta_1 - \theta_2))}{\sqrt{r_1^2 + r_2^2 - 2r_1 r_2 \cos(\theta_1 - \theta_2)}^3}\right],\\
\dot{p}_{\theta_i} &= -\frac{\delta^3 m_1 m_2 r_1 r_2 \sin(\theta_1 - \theta_2)}{\sqrt{r_1^2 + r_2^2 - 2r_1 r_2 \cos(\theta_1 - \theta_2)}^3},\\
\dot{p}_{\theta_2} &= \frac{\delta^3 m_1 m_2 r_1 r_2 \sin(\theta_1 - \theta_2)}{\sqrt{r_1^2 + r_2^2 - 2r_1 r_2 \cos(\theta_1 - \theta_2)}^3}.
\end{aligned} \tag{5.28}$$

We now aim to solve system (5.28).

5.3.2 Phase Condition and b Parameter

Consider the p_{θ_i} equations above. Any solution of system (5.28) which has $\sin(\theta_1 - \theta_2) \equiv 0$ for all time will necessarily have $p_{\theta_i} = const$, $i = 1, 2$. Requiring this restriction implies $\theta_1 - \theta_2 = n\pi$

for some $n \in \mathbb{Z}$ and for all time. When n is even, the asteroids have equal phase relative to the barycenter, meaning they are on the same side of the primaries. We determined numerically that this behavior leads to a collision between the asteroids. However, when n is odd, the asteroids have opposite phase, meaning they are diametrically opposed relative to the primaries, and there exist non-collision solutions.

In the odd case it is sufficient to study $n = 1$; we impose $\theta_1 - \theta_2 = \pi$. As discussed, this implies that $p_{\theta_i} = c_i$ for some constants $c_i \in \mathbb{R}$. The phase condition also implies that $\dot{\theta}_1 = \dot{\theta}_2$ for all time. That is, by Eqn. (5.28),

$$-\frac{2\pi}{P} + \frac{\delta^3 p_{\theta_1}}{m_1 r_1^2} = -\frac{2\pi}{P} + \frac{\delta^3 p_{\theta_2}}{m_2 r_2^2} \implies \left(\frac{r_1}{r_2}\right)^2 = \frac{c_1/m_1}{c_2/m_2} = \left(\frac{c_1}{c_2}\right)\left(\frac{m_2}{m_1}\right) > 0.$$

Immediately this implies $r_1/r_2 = const.$, and c_1 and c_2 must have the same sign (because of course $m_1, m_2 > 0$). Define

$$b = \sqrt{\frac{c_1/m_1}{c_2/m_2}} > 0, \tag{5.29}$$

so that the above work forces $r_1 = b r_2$ for all time.

We investigate circular periodic solutions in the regime wherein $r_i = const$. In this case, we have $\dot{r}_i = 0$, implying $p_{r_i} = 0$ once we solve Eqn. (5.28) for the radial momenta. Since the phase condition gives us that $\cos(\theta_1 - \theta_2) = \cos(\pi) = -1$, this in turn gives

$$0 = \dot{p}_{r_1} = \frac{\delta^3 m_1}{r_2^2}\left[\frac{b(c_2/m_2)^2}{r_2} - \frac{M}{b^2} - \frac{m_2}{(1+b)^2}\right].$$

Similarly,

$$0 = \dot{p}_{r_2} = \frac{\delta^3 m_2}{r_2^2}\left[\frac{(c_2/m_2)^2}{r_2} - M - \frac{m_1}{(1+b)^2}\right].$$

We can eliminate r_2 and the angular momentum c_2 from these equations if we divide each equation by $\delta^3 m_i/r_2^2$, multiply the $\dot{p}_{r_2}$ equation by b, and then subtract the $\dot{p}_{r_1}$ and $\dot{p}_{r_2}$ equations. Doing so

gives

$$\begin{aligned} 0 &= \left[\frac{b(c_2/m_2)^2}{r_2} - \frac{M}{b^2} - \frac{m_2}{(1+b)^2}\right] - \left[\frac{b(c_2/m_2)^2}{r_2} - Mb - \frac{m_1 b}{(1+b)^2}\right] \\ &= Mb + \frac{m_1 b}{(1+b)^2} - \frac{M}{b^2} - \frac{m_2}{(1+b)^2} \\ &= \frac{Mb^3(1+b)^2 + m_1 b^3 - M(1+b)^2 - m_2 b^2}{b^2(1+b)^2}. \end{aligned}$$

By setting the numerator to zero, dividing by M, and collecting like powers of b, we find that

$$q(b) = 0, \text{ where } q(z) = z^5 + 2z^4 + \left(1 + \frac{m_1}{M}\right) z^3 - \left(1 + \frac{m_2}{M}\right) z^2 - 2z - 1. \tag{5.30}$$

5.3.3 Analysis of b Parameter

For most values of m_1, m_2, and M, we cannot factor the real polynomial $q(z)$ from Eqn. (5.30) since it is a quintic. However, since the masses are all positive, we can analyze its roots. Descartes' Rule of Signs says that in this case, there is exactly one positive real root, for there is one sign change in the sequence of coefficients of $q(z)$. Since $b > 0$, it must be the one positive root.

In addition, we see that $q(0) = -1$, $q(z) \to \infty$ as $z \to \infty$, and $q(1) = (m_1 - m_2)/M$. By continuity of q, we may therefore invoke the Intermediate Value Theorem to place b within $(0, \infty)$ according to the relative sizes of m_1 and m_2:

$$b \in \begin{cases} (0,1) & \text{if } m_1 > m_2 \\ \{1\} & \text{if } m_1 = m_2 \\ (1,\infty) & \text{if } m_1 < m_2 \end{cases}. \tag{5.31}$$

In particular, $m_1 = m_2$ forces $r_1 = r_2$ (and $c_1 = c_2$), in accordance with the COM approach which says $x_1 = -x_2$, etc.

In practice, we must obtain b numerically once values of m_1, m_2, and M are fixed. We found that for all realistic masses (e.g., when $m_1, m_2 \leq M$), b remains close to 1 (see Figure 5.1). To get

$b > 2$ or $b < 0.5$, we find that the mass ratios $\mu_i = m_i/M$ need to be on the order of 20, which is extremely unrealistic.

Figure 5.2 shows the extreme case of a comet orbit with $b = 2$, to better demonstrate the effect on the asteroid trajectories. For more realistic asteroid masses, the effect is too small to observe on these graph scales.

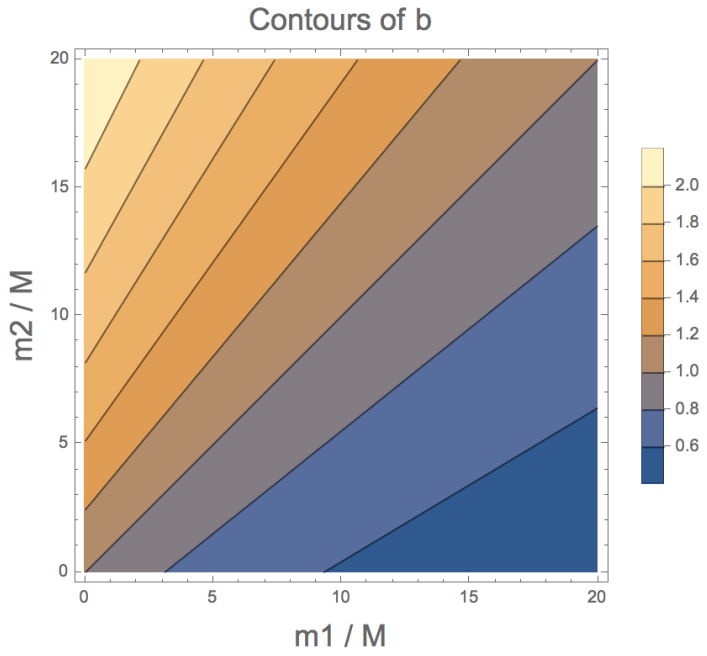

Figure 5.1 Contours showing the value of b as a function of the input mass ratios m_1/M and m_2/M.

5.3.4 Solution and Continuation

Once b is determined, we can solve for r_2 in the $\dot{p}_{r_2}$ equation:

$$0 = \frac{(c_2/m_2)^2}{r_2} - M - \frac{m_1}{(1+b)^2} \implies r_2 = \frac{(1+b)^2(c_2/m_2)^2}{M(1+b)^2 + m_1}.$$

Some algebraic manipulation involving the use of $q(b) = 0$ reveals

$$r_1 = br_2 = \frac{(1+b)^2(c_1/m_1)^2}{M(1+b)^2 + m_2 b^2}.$$

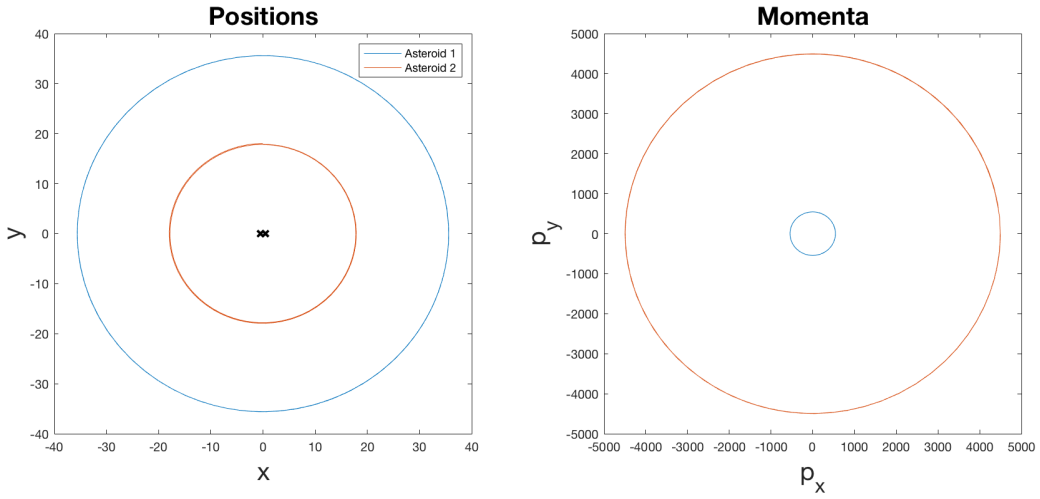

Figure 5.2 A comet solution of (5.28) with $b = 2$ and $\delta = 1$. To obtain this b, we had to use extremely large (and thus unrealistic) asteroid masses.

We may also obtain $\dot{\theta}_i$, which happens to be constant:

$$\dot{\theta}_i = \omega = -\frac{2\pi}{P} + \frac{\delta^3[M(1+b)^2+m_1]^2}{(1+b)^4(c_2/m_2)^3} = -\frac{2\pi}{P} + \frac{\delta^3[M(1+b)^2+m_2b^2]^2}{(1+b)^4(c_1/m_1)^3}. \tag{5.32}$$

Hence we have obtained a periodic circular solution to (5.28):

$$\begin{aligned}
r_1(t) &= br_2 = \frac{(1+b)^2(c_1/m_1)^2}{M(1+b)^2+m_2b^2}, & r_2(t) &= \frac{(1+b)^2(c_2/m_2)^2}{M(1+b)^2+m_1},\\
\theta_1(t) &= \pi+\theta_0+\omega t, & \theta_2(t) &= \theta_0+\omega t,\\
p_{r_1}(t) &= 0, & p_{r_2}(t) &= 0,\\
p_{\theta_1}(t) &= c_1 = \frac{m_1}{m_2}b^2c_2, & p_{\theta_2}(t) &= c_2.
\end{aligned} \tag{5.33}$$

The period is simply $T = 2\pi/|\omega|$.

To continue this solution into the Binary Asteroid Problem, we need to compute the multipliers. Since we haven't implemented any reductions to the degrees of freedom, we will have to work with an 8×8 monodromy matrix $\mathfrak{M}$. As in Section 5.1.3, we still have

$$\mathfrak{M} = \exp\left(T\cdot J_2D^2(H_0+\delta^3H_3)\right), \tag{5.34}$$

but now the variables correspond to those defined in this section. We have

$$J_2D^2(H_0+\delta^3H_3)=\begin{bmatrix}-A^T & B\\ C & A\end{bmatrix} \tag{5.35}$$

in block form, where the blocks are

$$A=\begin{bmatrix}0 & A_1/b & 0 & 0\\ 0 & 0 & 0 & 0\\ 0 & 0 & 0 & A_1\\ 0 & 0 & 0 & 0\end{bmatrix},\quad B=\begin{bmatrix}B_1 & 0 & 0 & 0\\ 0 & B_2 & 0 & 0\\ 0 & 0 & B_3 & 0\\ 0 & 0 & 0 & B_4\end{bmatrix},\quad C=\begin{bmatrix}C_{11} & 0 & C_{13} & 0\\ 0 & C_{22} & 0 & -C_{22}\\ C_{13} & 0 & C_{33} & 0\\ 0 & -C_{22} & 0 & C_{22}\end{bmatrix}, \tag{5.36}$$

and the time-independent entries are given by

$$A_1=\frac{2\delta^3(c_2/m_2)}{r_2^3},\qquad B_1=\frac{\delta^3}{m_1},\qquad B_2=\frac{\delta^3}{m_1b^2r_2^2},\qquad B_3=\frac{\delta^3}{m_2},\qquad B_4=\frac{\delta^3}{m_2r_2^2},$$

$$\begin{aligned}C_{11}&=-\frac{\delta^3m_1[M(1+b)^2+m_2b^2(3+b)]}{b^3(1+b)^3r_2^3}, & C_{13}&=\frac{2\delta^3m_1m_2}{(1+b)^3r_2^3},\\ C_{33}&=-\frac{\delta^3m_2[M(1+b)^3+m_1(1+3b)]}{(1+b)^3r_2^3}, & C_{22}&=\frac{\delta^3m_1m_2b}{(1+b)^3r_2}.\end{aligned} \tag{5.37}$$

Mathematica gave the characteristic polynomial of (5.35) as being of the form

$$\det\left(J_2D^2(H_0+\delta^3H_3)-zI\right)=D_1z^2+D_2z^4+D_3z^6+z^8.$$

We are interested in D_1 only, but for completeness the coefficients are:

$$\begin{aligned}D_1&=B_1B_3C_{22}\left[-\frac{A_1^2}{b^2}\left(b^2C_{11}+2bC_{13}+C_{33}\right)+(B_2+B_4)\left(C_{13}^2-C_{11}C_{33}\right)\right]\\ D_2&=C_{22}\left[\frac{A_1^2}{b_2}\left(B_1+b^2B_3\right)+(B_2+B_4)(B_1C_{11}+B_3C_{33})\right]-B_1B_3\left(C_{13}^2-C_{11}C_{33}\right),\\ D_3&=-\left[B_1C_{11}+(B_2+B_4)C_{22}+B_3C_{33}\right].\end{aligned} \tag{5.38}$$

Recall from Section 5.1.3 that the eigenvalues of $\mathfrak{M}$ are $\lambda=e^{zT}$ where z represents an eigenvalue of $J_2D^2(H_0+\delta^3H_3)$. Therefore, showing that $+1$ is a multiplier exactly twice is equivalent to showing

0 is an eigenvalue of $\det\left(J_2D^2(H_0+\delta^3H_3)-zI\right)$ exactly twice. From the characteristic polynomial above, this amounts to showing $D_1 \neq 0$.

Note that B_1, B_3, and C_{22} are each positive, so it is sufficient to examine $D_1/(B_1B_3C_{22})$. We claim it is positive, and write it in terms of δ, M, b, r_2, and the asteroid mass ratios $\mu_i = m_i/M$. With some manual factoring and through the use of $q(b)=0$, Mathematica gives that $D_1/(B_1B_3C_{22})$ is expressible as

$$\begin{aligned}
\frac{D_1}{B_1B_3C_{22}} &= \frac{\delta^9M^3}{b^5(1+b)^4r_2^8}\left[k_0+k_1b+k_2b^2+k_3b^3+k_4b^4\right], \text{ where} \\
k_0 &= 6\mu_1+3\mu_2+\mu_1\mu_2, \\
k_1 &= 15\mu_1+12\mu_2+3\mu_1\mu_2, \\
k_2 &= 15\mu_1+18\mu_2+11\mu_1\mu_2+3\mu_1^2+\mu_2^2-\mu_1\mu_2^2, \\
k_3 &= 9\mu_1+12\mu_2+8\mu_1\mu_2-2\mu_1^2+4\mu_2^2+2\mu_1^2\mu_2+3\mu_1\mu_2^2, \\
k_4 &= 3\mu_1+3\mu_2+2\mu_1\mu_2-2\mu_1^2+3\mu_2^2-2\mu_1^2\mu_2. \qquad (5.39)
\end{aligned}$$

We use this information to complete the continuation argument.

Theorem 8. ***(Periodic Comet Orbits)*** *For almost every choice of realistic masses m_1, m_2, M_1, M_2 (meaning $m_1, m_2 \leq M$), there exist two one-parameter families of near-circular periodic solutions to the Binary Asteroid Problem* (2.18)*, where the asteroids orbit far away from the primaries, on tracks diametrically opposed to each other. The parameter is the symplectic scale factor $\delta > 0$ and the families are characterized by having positive or negative angular momentum.*

Proof. Every quantity (except possibly k_2, k_3, k_4) in (5.39) is clearly positive. There are values of μ_1, μ_2 which make k_2, k_3, and/or k_4 negative, but because we have $\mu_1, \mu_2 \in (0,1]$ by the realism

hypothesis, we see

$$k_2 \geq 15\mu_1 + 18\mu_2 + 10\mu_1\mu_2 + 3\mu_1^2 + \mu_2^2 > 0,$$
$$k_3 \geq 7\mu_1 + 12\mu_2 + 8\mu_1\mu_2 + 4\mu_2^2 + 2\mu_1^2\mu_2 + 3\mu_1\mu_2^2 > 0,$$
$$k_4 \geq \mu_1 + 3\mu_2 + 3\mu_2^2 > 0.$$

Therefore, because $b > 0$, we have $k_0 + k_1 b + k_2 b^2 + k_3 b^3 + k_4 b^4 > 0$ and hence $D_1 > 0$.

It must be that 0 is an eigenvalue of $J_2 D^2(H_0 + \delta^3 H_3)$ exactly twice. Furthermore, because $J_2 D^2(H_0 + \delta^3 H_3)/\delta^3$ is independent of δ according to Eqns. (5.36) and (5.37), it follows that the remaining nonzero eigenvalues are all δ^3 times some constant.

Therefore, the multipliers of the periodic solution (5.33) to $H_0 + \delta^3 H_3$ are of the form

$$\lambda = e^{zT} = \exp\left(\frac{\delta^3}{h_1 + h_2\delta^3}\right) = 1 + O(\delta^3).$$

The argument of Theorem 6 applies to conclude (5.33) continues into a periodic solution to the Binary Asteroid problem. □

The process of comet continuation is shown in Fig. 3.2. Unlike the Hill and central-Hill continuations, the comet orbits become tighter and tighter as δ increases.

Chapter 6

Remarks and Conclusion

We have thus presented a Hamiltonian model for the dynamics of two small, positive mass asteroids in the gravity of two known primaries. According to Chapter 4, the dynamics of our model are similar to those seen in the classical CR3BP. One way to summarize the relationship is that our problem is like two CR3BPs stitched together. This intuition led us to the Lagrange point relative equilibria and to periodic orbits of Hill and comet type, each of which is also present in the CR3BP.

Our model does have its own distinctive features, however. The periodic central-Hill orbits of Chapter 5 are the prime example of this. In fact, among the results presented in this work, the central-Hills are the best representatives of what the term "binary asteroid" typically means in astronomy. According to Fig. 3.5, the term should refer to the asteroids being gravitationally bound to each other. In short, the asteroids would behave as one particle as they move in the field of the primaries. One objective for future work is to find more of these binary type orbits.

Another objective for future study is to extend our results to the full three-dimensional case. The Hamiltonian H_{BA} is easily adapted to this more general setting; we omitted it in this work because it adds much more complexity both to the derivations of Chapter 2 and to the equations of motion in the subsequent chapters. Some preliminary investigations have revealed the numerical possibility of the extension of our main results, however, there does not seem to be a simple method of adapting

the proofs.

6.1 Binary Type Orbits

The COM coordinates of Eqn. (2.22) can be adapted for use in the full 4-body problem with arbitrary masses m_1, m_2, M_1, and M_2 are all arbitrary, and in doing so they provide a suitable system for analyzing binary type orbits. When the relative positions x and y are small, the asteroids are close, and their aggregate motions are essentially tracked by the COM variables α and β.

One method for finding periodic binary type orbits in this setup is similar to what was performed in Chapter 5.2: shift the α and β variables so that $(\alpha, \beta) = (0,0)$ corresponds to a relative equilibrium of the amended potential of the primaries. Then perform a scaling $x' = \delta^n x$, $y' = \delta^n y$ for a small $\delta > 0$ and a yet unknown power $n > 0$. Finally, we expand the Hamiltonian in a Taylor series in δ and see if any truncation of that Taylor series is itself a solvable Hamiltonian system.

In a future work, we will present present periodic solutions to the full 4-body problem where the asteroids orbit each other around any of the collinear Lagrange points discussed in this thesis. These orbits are exactly analogous to the central-Hills, the only difference being the locations of the asteroids.

Intuition suggests that binary type orbits should also exist at the equiliateral triangle equilibria L_4 and L_5. However, the techniques used in finding the binary orbits at the collinear orbits do not extend to L_4 and L_5. We believe that part of the issue is the possible presence of multiple trapezoidal "convex" relative equilibria, discussed in Corbera, Cors, & Roberts [10]: their closeness might cause chaotic dynamics.

Nevertheless, there may be at least quasi-periodic orbits near L_4 and L_5. Figure 6.1 displays a numerical simulation of the rotating 4-body problem with initial conditions near an L_4 configuration. Although the asteroids eventually drift away from L_4 and break their binary character, they move as

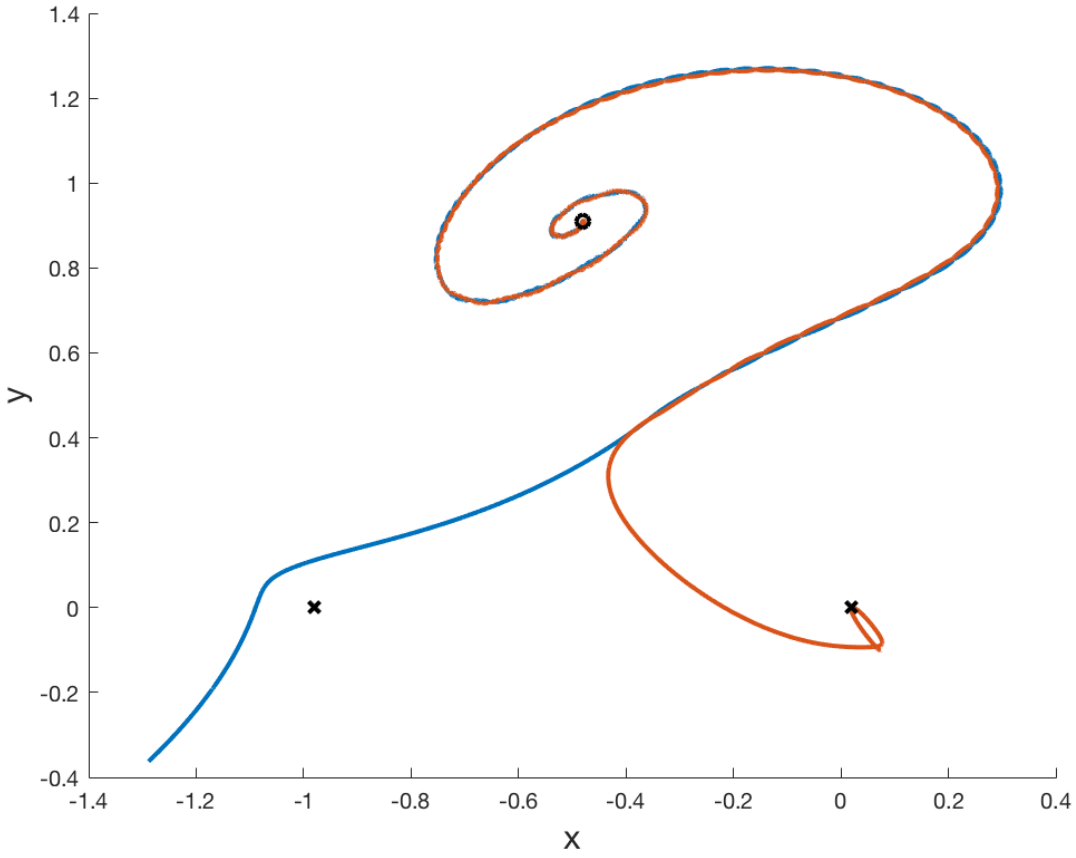

Figure 6.1 Numerical simulation of the 4-body problem in the rotating coordinates of Section 2.1.1. The asteroids follow the blue and red tracks. The primaries' motions are very slight, but their approximate locations are marked with black x's. The black open circle is the L_4 equilibrium point.

one unit for a relatively long time. The time displayed in Fig. 6.1 is 243 times the would-be period of a corresponding central-Hill orbit. By contrast, in the first 10 periods, these asteroids remain very close to L_4, whence our hypothesis that some kind of L_4 binary orbits exist.

6.2 3-D Orbits

Similar to how the Moon orbits the Earth outside of the plane defined by the Earth-Sun orbit, we can expect there to be bounded 3-D orbits for binary asteroids. To derive a full 3-D Binary Asteroid Hamiltonian, we simply repeat the derivation of Section 2.2.1 with some modifications to account for a third dimension. The primaries are assumed to move only in the xy-plane, while the asteroids are allowed to move in any of the x, y, and z directions.

Figure 6.2 displays an example of such an orbit. Notice that the trajectories are not simple elliptical rings like in the 2-D case. This adds to the difficulty of their analytical calculation. However, in the tracks in Fig. 6.2, we remark that the asteroids remain on fixed, bounded ellipsoidal shells, so the dynamics are not too complicated.

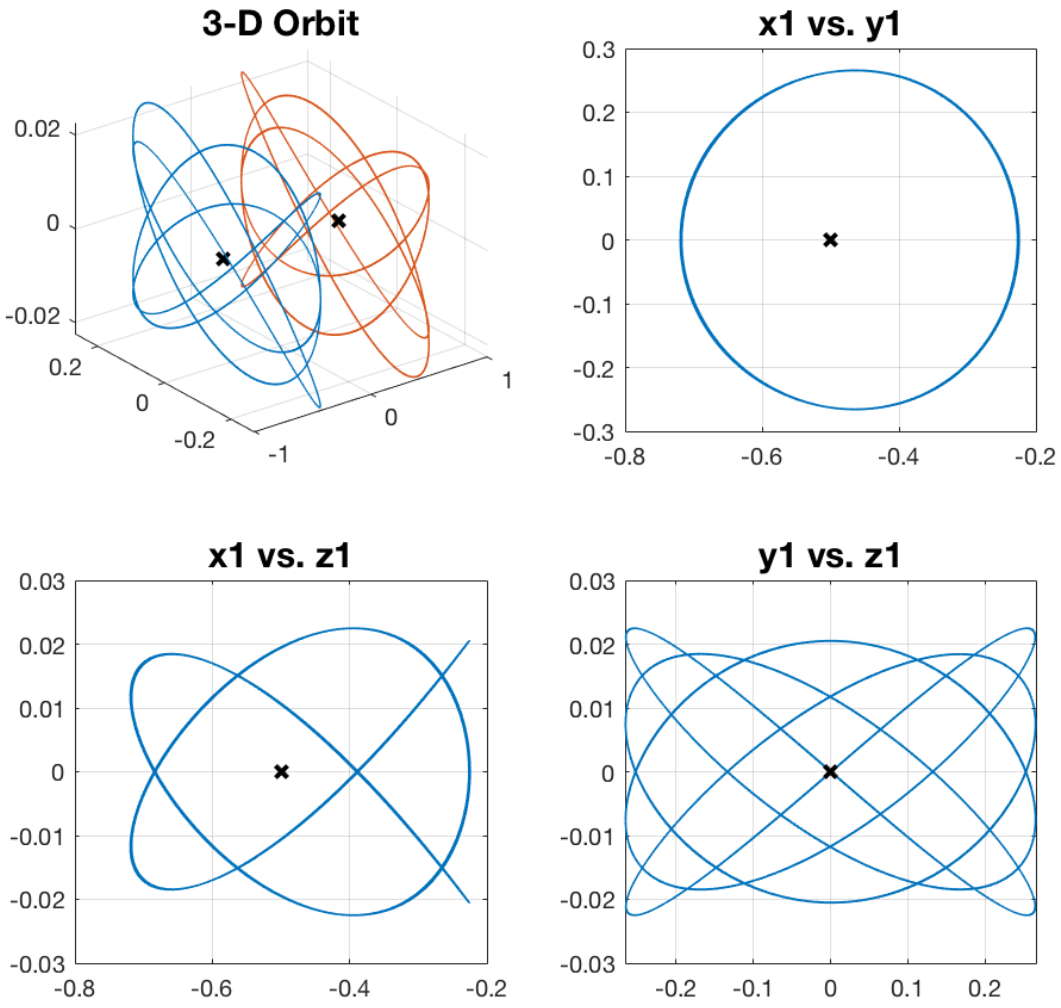

Figure 6.2 Depiction of a 3-D Hill orbit in the Binary Asteroid problem. The top left graph shows the trajectories of both asteroids (blue and red) about the primaries (black x's). The remaining graphs are cross-sections of the orbit of the blue asteroid.

Bibliography

[1] K. R. Meyer and D. C. Offin, *Introduction to Hamiltonian Dynamical Systems and the N-Body Problem*, Vol. 90 of *Applied Mathematical Sciences*, 3rd ed. (Springer International Publishing, 2017).

[2] J. R. Taylor, *Classical Mechanics* (University Science Books, 2005).

[3] W. R. Hamilton, *On a general method of expressing the paths of light, & of the planets, by the coefficients of a characteristic function* (P.D. Hardy, Dublin, Ireland, 1833).

[4] J. Davis, "Planetary Society asteroid hunters help find rare type of double asteroid," https://www.planetary.org/articles/shoemaker-winners-2017-ye5 (Accessed March 4, 2023).

[5] P. A. Taylor *et al.*, "Radar and Optical Observations of Equal-Mass Binary Near-Earth Asteroid (190166) 2005 UP156," In *51st Annual Lunar and Planetary Science Conference*, Lunar and Planetary Science Conference p. 2333 (2020).

[6] DART mission overview webpage, https://dart.jhuapl.edu/Mission/index.php (Accessed April 11, 2023).

[7] A. S. Rivkin *et al.*, "The Double Asteroid Redirection Test (DART): Planetary Defense Investigations and Requirements," The Planetary Science Journal 2 (2021).

[8] J. Llibre, D. Paşca, and C. Valls, "The circular restricted 4-body problem with three equal primaries in the collinear central configuration of the 3-body problem," Celestial Mechanics and Dynamical Astronomy 133 (2021).

[9] M. Alvarez-Ramírez, J. Skea, and T. Stuchi, "Nonlinear stability analysis in a equilateral restricted four-body problem," Astrophys Space Sci 358 (2015).

[10] M. Corbera, J. M. Cors, and G. E. Roberts, "Classifying four-body convex central configurations," Celestial Mechanics and Dynamical Astronomy 131 (2019).

[11] G. E. Pollock IV and J. A. Vedda, "Cislunar Stewardship: Planning for Sustainability and International Cooperation," (2020).

[12] L. F. Bakker and N. J. Freeman, "Relative Equilibria and Periodic Orbits in a Binary Asteroid Model," In progress (2023).

[13] G. W. Hill, *The Collected Mathematical Works of George William Hill* (Carnegie Institution of Washington, 1905), Vol. 1.

Index